Delivery Performance of Conventional Aircraft by Terminal-Area, Time-Based Air Traffic Control

A Real-Time Simulation Evaluation

Leonard Credeur,
Jacob A. Houck,
William R. Capron,
and Gary W. Lohr

NASA

Delivery Performance of Conventional Aircraft by Terminal-Area, Time-Based Air Traffic Control

A Real-Time Simulation Evaluation

Leonard Credeur
and Jacob A. Houck
Langley Research Center
Hampton, Virginia

William R. Capron
PRC Kentron, Inc.
Aerospace Technologies Division
Hampton, Virginia

Gary W. Lohr
Embry-Riddle Aeronautical University
Daytona Beach, Florida

Contents

Symbols and Abbreviations

ARTS	automated radar terminal system
ATC	air traffic control
ATIS	automatic terminal information service
ATOPS	Advanced Transport Operating Systems
Avg	average
CAS	calibrated airspeed
CDT	command delivery time
CRT	cathode ray tube
DEN	Denver's Stapleton International Airport (or Denver Vortac)
DICE	direct-course error
ETA	estimated time of arrival
FAA	Federal Aviation Administration
FMS	flight management system
$\dot{H}$	rate of descent, ft/sec
IAS	indicated airspeed
IFR	instrument flight rules
ILS	instrument landing system
IMC	instrument meteorological conditions
L	left
MOTAS	Mission-Oriented Terminal-Area Simulation
MSL	mean sea level
n	number of cases
O.M., OM	outer marker
PPI	plan position indicator
RWY	runway
SLT	scheduled landing time
TAATM	terminal-area air traffic model
TIMER	traffic intelligence for the management of efficient runway scheduling
t	response time
t'	transformed response time
VAR	variation of the Earth's magnetic field
x, y, z	Cartesian coordinate system
α	percent of significance of F test
β	shape parameter of Weibull distribution
γ	location or threshold parameter of Weibull distribution
η	scale parameter of Weibull distribution
μ	mean value
σ	standard deviation
σ_c	standard deviation of controller's message-delivery-time error relative to TIMER expected delivery time
σ_d	runway delivery-time-error standard deviation for a single aircraft
σ_i	runway interarrival-time-error standard deviation for an aircraft pair
σ_p	pilot-in-the-loop/TIMER algorithm, time-error standard deviation for a single aircraft
4D	four-dimensional (x, y, z, and time)

v

Summary

A real-time simulation study was conducted of a time-based, extended-terminal-area air traffic control (ATC) concept called traffic intelligence for the management of efficient runway scheduling (TIMER). The principal objective of the study was to measure, under realistic full-workload conditions, the performance and reaction of flight crews flying TIMER-assisted approaches in a conventional electromechanical cockpit without cathode ray tube (CRT) displays or a four-dimensional (4D) flight management system. Additional experimental objectives were to verify earlier fast-time TIMER study results and to obtain data for the validation or refinement of computer models of pilot/airborne performance. A real-time ATC simulation with the TIMER algorithm embedded was linked to a DC-9 cockpit simulator. These facilities together with a certified ATC controller, pseudo pilot, and subject professional airline crews formed the basis for a total system simulation for realistic crew-in-the-loop experiments.

Previous TIMER fast-time results in NASA TP-2870 indicated a runway-threshold, interarrival-time-error standard deviation of about 12 sec for pairs of non-4D aircraft with computer aiding and knowledge of the aircraft final-approach speed. As a point of reference, a report by Martin and Willett in 1968 measured 26.5 sec for the interarrival-time-error standard deviation of manual control with no computer aiding. Based on the measured real-time, piloted-simulation delivery error at the runway threshold, a system interarrival-time-error standard deviation was determined to be in the range of 10.4 to 14.1 sec. This real-time outcome supports the 12 sec predicted by earlier TIMER fast-time simulations and demonstrated the evolutionary features of the concept. (That is, the concept bridges the gap between conventional aircraft cockpits having a manual voice-linked ATC system and advanced aircraft cockpits in a data-link environment with further ground automation.) Other real-time system performance parameters measured include approach speeds, response time to controller's turn instructions, bank angles, and ATC controller's message-delivery-time errors. These data will enable ATC researchers to verify and refine computer models of the pilot/airborne system and the controller's performance.

1.0 Introduction

A description and a detailed fast-time evaluation of a time-based, extended-terminal-area air traffic control (ATC) concept called traffic intelligence for the management of efficient runway scheduling (TIMER) was presented in reference 1. The results identified and showed the effects and interactions of key system variables. The TIMER concept was designed for evolutionary integration into the manual, voice-linked ATC system and for handling both four-dimensional (4D) flight management system (FMS) equipped aircraft and non-4D-equipped aircraft. As was stated in reference 1, it is anticipated that when a terminal-area, time-based ATC system is first introduced, many, if not most, of the aircraft will not be equipped with a terminal-compatible 4D FMS. Until most of the aircraft are equipped with a flexible, terminal-compatible 4D FMS, the performance of a time-based system will be constrained by non-4D aircraft performance. Thus, the runway delivery-time performance precision achievable with conventional aircraft not equipped with 4D FMS is a key issue relating to the system capacity of an initial terminal-area, time-based flow control system such as TIMER.

Fast-time simulation results (ref. 1) indicated that with computer aiding, which has aircraft final-approach-speed information, a runway interarrival-error standard deviation of about 12 sec could be achieved for non-4D traffic. As a point of reference, a field study (ref. 2) conducted by the Federal Aviation Administration (FAA) in New York measured 26.5 sec for the interarrival-error standard deviation of manual control with no computer aiding. One of the objectives of this study was to validate the fast-time results by assessing the performance and reaction of flight crews under realistic full-workload conditions when flying a TIMER-assisted approach in a conventional electromechanical cockpit without a 4D FMS. Another objective was to obtain data on pilot/aircraft performance so that computer models, used in TIMER and other ATC simulations, could be validated or refined. The primary area of interest is the final-approach performance in a TIMER environment.

Several facilities were integrated and used to conduct the simulation study. The real-time version of the terminal area air traffic model (TAATM) described in reference 3 with the TIMER algorithm embedded was linked to a DC-9 cockpit simulator via the Langley Mission-Oriented Terminal-Area Simulation (MOTAS) Facility. Additional facilities included controller work stations, a voice communication link, and a landing-scene generator. These facilities together with a certified ATC controller, pseudo pilot, and professional airline crews as subjects formed the basis of a total system simulation for real-time crew-in-the-loop experiments.

Several simulated instrument flight rules (IFR) approaches, based on a runway 26L configuration at Denver's Stapleton International Airport, were flown

from two different routes by each of the airline crews. A series of data runs were conducted with each crew requested to react to controller instructions as they normally would on an IFR approach. Each crew was then briefed on the TIMER concept and how it was being applied; then another series of simulated approaches were performed and the differences were compared. TIMER operations and controller activities were the same for both series of data runs. The runway-threshold error of each approach was measured as well as the pilot/aircraft system response to speed and turn commands. Individual crew reactions were obtained via questionnaires and comments.

2.0 TIMER Concept Overview

2.1 TIMER Concept Features

TIMER is an extended-terminal-area flow control concept that begins its control in en route airspace at the horizon of control. The major operational features of the TIMER concept are shown in figure 1. The principal features are summarized as follows:

1. The arrival stream into the extended terminal area is derandomized at the horizon of control by establishing a proposed aircraft landing sequence and building a list of aircraft scheduled landing times (SLT's) based on separation criteria (events ① and ② of fig. 1). The desired metering-fix time as a result of the assigned landing time is also determined.

2. Nominal estimated times of arrival used in step 1 are based on representative aircraft performance models. From using these models and predicted winds, a ground-computed trajectory is determined to meet the aircraft assigned scheduled landing time (events ③ and ④ of fig. 1).

3. Computer-generated assistance is given to the controller to help him meet aircraft target times based on the trajectory calculations. The parameters determined are the en route cruise speed, the time to initiate as well as the Mach/CAS speeds to fly a flight-idle-thrust descent, and the terminal segment speeds and headings.

4. Adjustments to the scheduled landing times and, if necessary, changes in the landing sequence are made to accommodate errors and anomalies in factors such as wind, navigation, airspeed, and heading which affect the SLT of either the own aircraft or the preceding aircraft. These schedule adjustments or controller-action points occur at the following points shown in figure 1: the metering fix, the speed adjustment points, and the fine-tuning region. The landing sequence is fixed before aircraft arrive in the fine-tuning region.

5. The aircraft trajectory is fine tuned in the final-approach region in order to meet the aircraft final scheduled landing time with limited time error. The performance in the final-approach fine-tuning region is the primary focus of this paper.

A more complete description of the TIMER concept is furnished in reference 1. References 4 through 9 describe some of the recent, closely related research and development activity in the area of extended-terminal-area, time-based air traffic control.

2.2 Fine-Tuning Region

The TIMER fine-tuning region is defined by the boundaries of the vector heading from the aim point for the eastern arrivals (event ⑥ in fig. 1) and by the boundaries of the downwind-to-base turn for the western arrivals (event ⑤ in fig. 1). The dashed lines in both figures 1 and 2 indicate the boundaries of the fine-tuning region. Within this region the computer-aided fine-tuning maneuvers consist of timing both the turn-to-base maneuver (event ⑤ in fig. 1) and the turn-to-final maneuver (event ⑦). In keeping with the evolutionary nature of the TIMER concept, the design was configured to be similar in geometry and procedures to the conventional approach performed today. That is, the pilot would not be able to distinguish between a TIMER-assisted final approach and a conventional radar, manual-controlled approach.

The fine-tuning process is based on a regularly updated, estimated time of arrival (ETA) calculation that displays how early, relative to its SLT, the aircraft would be if its turn instructions were issued immediately. The difference between the SLT and the ETA is referred to as the direct-course error (DICE) value. DICE gives more information than a straight clock countdown display that indicates only the remaining time to issue the turn command. With expected communication and response times of both the controller and pilots factored in, the data tag of each aircraft on the controller display is enhanced to indicate when, and to what heading, the controller would vector the aircraft for the base and localizer intercept segments. The fine-tuning region must accommodate minor schedule changes due to other aircraft errors, wind estimate errors, or own aircraft flight errors that have accumulated since the last speed control point.

3.0 Experimental System

3.1 Experimental Facilities

A complex system simulation using the Denver Stapleton approach routes was assembled to provide

a realistic and dynamic environment for measuring crew-in-the-loop, aircraft approach performance in a TIMER environment. A real-time version of the terminal-area air traffic model (TAATM) with the TIMER algorithms embedded interacted with a certified ATC controller by means of a controller station and plan position indicator (PPI) to provide the ATC environment and scenarios. The Langley DC-9 Full-Workload Simulator cockpit provided the vehicle for airline crew interaction. The computer data interfaces, voice links, and controller workstations of the Langley Mission-Oriented Terminal-Area Simulation (MOTAS) Facility (ref. 10) linked the TIMER algorithms and cockpit simulator interactively.

3.1.1 Mission-Oriented Terminal-Area Simulation

The Langley Mission-Oriented Terminal-Area Simulation (MOTAS) Facility shown in figure 3 (and discussed in ref. 10) is a sophisticated system simulation capability that provides an environment in which research studies can be conducted in flight management and flight operations with a high degree of realism. This facility provides a flexible and comprehensive simulation of the airborne, ground-based, and communications aspects of the airport terminal-area environment. The major elements of the MOTAS facility are an airport terminal-area environment model, several aircraft models and simulator cockpits, four pseudo-pilot stations, two air traffic controller stations, and a realistic air/ground communications network. In addition, the MOTAS facility can be linked to the NASA Wallops Flight Facility at Wallops Island, Virginia, by telephone data communication lines or satellite to allow interaction with live aircraft for actual flight tests. The airport terminal-area environment model gives a current representation of Denver's Stapleton International Airport and surrounding area using either the TIMER automation aids to the controller or present-day manual control. In addition, the model simulates radar systems, navigation aids, wind conditions, etc.

The MOTAS facility combines the use of several aircraft cockpit simulators and pseudo-pilot stations for flying aircraft in the simulated airport terminal area. The facility is presently operational with the Transport Systems Research Vehicle (TSRV) Simulator, the General Aviation Simulator, and the DC-9 Full-Workload Simulator. These aircraft cockpit simulators allow entire crews to fly realistic missions in the airport terminal area. Simulated aircraft can also be controlled through the use of the pseudo-pilot stations. The operators of these stations can handle up to 15 aircraft simultaneously by inputting control commands to change airspeed, altitude, direction,

etc. The final major component of the facility is the air traffic controller stations, which are described in section 3.1.3.

3.1.2 The DC-9 Full-Workload Simulator

The transport aircraft cockpit (fig. 4) used in this study was a fixed-base full-workload simulator outfitted as a DC-9 aircraft. A television model board (fig. 5) provided the out-of-window landing scene for the crew, which included visibility effects and approach lighting systems used to simulate Category I landing conditions for this study (ref. 11). The aircraft dynamics modeled were those of the McDonnell Douglas DC-9 Series 30 aircraft. A full complement of cockpit electromechanical instruments was provided, with all major systems functional including autopilot, dual flight directors, and navigation and communication radios. Subsystems, such as hydraulics and electrical systems, were modeled to the extent necessary to provide normal in-flight operations and readouts to the crew.

The aircraft cockpit and terminal-area simulation programs were run simultaneously on separate Control Data CYBER 175 computer systems that communicated with each other through extended core storage. This allowed various aircraft data, such as x, y, z positions, airspeed, bank angle, etc., from the DC-9 program to be sent to the terminal-area program for processing. The multifrequency radio communications were simulated with selectable voice-link channels between the cockpit radio tuning heads and the ATC controller's radar display consoles of the terminal-area simulation.

3.1.3 Simulation Air Traffic Controller Stations

The air traffic controller's interaction to the cockpit was provided using the facilities of the Mission-Oriented Terminal-Area Simulation (MOTAS). The MOTAS components used for the simulation are described below.

As shown in figure 6, two controller stations (ATC stations 1 to the left and 2 to the right) were equipped with a plan position indicator (PPI) on which aircraft position information is displayed. Each station had a communications system for the verbal exchange of information between the controller, the subject aircraft (DC-9 cockpit), and the pseudo pilot as indicated in figure 7. Additionally, ATC station 2 is equipped with an electronic data tablet for interaction with TIMER-generated commands that appear on the PPI.

The controller displays are simulated by an Evans & Sutherland Multi Picture System with a CRT measuring 23 in. in diameter and mounted vertically (fig. 6). The display is configured with a video map of

the Denver terminal area (fig. 8). Status information for the instrument approach in use, the altimeter setting, and the automatic terminal information service (ATIS) code were presented in the lower portion of the display.

An aircraft position is indicated by an elongated delta symbol with two trailing chevrons that provide past-position information of the aircraft track. An associated alphanumeric data block is connected to the aircraft symbol with a leader line; the specifics of the alphanumeric data block are addressed in a later section.

Several components comprise the communications system. Both ATC stations are equipped with an audio control panel and four preset frequencies. The audio panels are the interface between the controller headsets and a switching system that searches for a match of the frequency selected at the controller stations and at the cockpit. A voice disguiser linked to the audio panel serving ATC station 1 (the left station in fig. 7) provided the capability for varying the voice output of that station, thus creating for the DC-9 cockpit the environment of different pilots responding to ATC commands.

3.2 Experimental Conditions and Interactions

3.2.1 Terminal-Area Conditions

The approach routes of Denver's Stapleton International Airport operating in a runway 26L landing configuration (fig. 2) were used assuming instrument meteorological conditions (IMC) weather procedures. In anticipation of real-time experiments with the ATOPS Boeing 737 research aircraft operating at the Wallops Flight Facility, the approach paths were modified in the TIMER to reflect the corresponding magnetic variation and altitudes at Wallops. Thus, the terminal-area altitudes were reduced by approximately 5000 ft from the Denver altitudes. The outer-marker intercept altitude and runway elevation were set to 1900 ft and 40 ft MSL, respectively, and the active runway was designated as 28L. Hereinafter, the simulated airport will be referred to as Denver/Wallops.

The area of interest in this study was the final-approach performance of the conventional electromechanical, non-4D-equipped aircraft in the TIMER environment. Since the southern approach routings (BYSON and KIOWA) are geometrically similar to the northern routings (DRAKO and KEANN), only the latter two were used for experimental data flights in the cockpit simulator. However, computer-simulated traffic controlled by TIMER was flown from all four approach routes.

A linear wind model using statistical coefficients for an average Denver area wind was used in all runs. The simulated wind velocity at ground level was 7.9 knots from 277° with a speed gradient of 2.368 knots per 1000 ft. In this study the wind direction was constant at all altitudes.

3.2.2 Approach Paths and Procedures

The expected flight paths for the two inbound routes used by the cockpit simulator in the study are depicted in the simplified approach charts shown in figures 9 and 10. The charts show applicable radio frequencies, nominal indicated airspeeds, magnetic headings, and MSL altitudes in the final-approach area. For each experimental flight either the DRAKO or KEANN approach was chosen from the subset of simulated DC-9 flights generated in a fast-time run under simulation conditions identical to those in the real-time experiment. Thus, the initial conditions for each approach within the subset were slightly different because of variations in assigned airspeeds and the error models in the TIMER program. Each crew used the same subset of initial conditions. The actual initialization points were selected to be 1 minute prior to either the turn to downwind on the DRAKO approaches or to the turn to base in the vicinity of the FLOTS intersection on the KEANN approaches.

The events that occurred during the approaches can be described by referring to the labeled areas in figure 11. For initialization (area I), the position, speed, heading, and descent rate of the simulated target aircraft were transmitted to the DC-9 simulation program via computer memory shared by the TIMER and DC-9 programs while the TIMER was put in a hold mode. After the aircraft simulator was aerodynamically trimmed and the two programs were returned to real-time operation mode, the pilot was expected to maintain the initial airspeed and to track inbound to the DEN VORTAC. There was an initial communication exchange between the cockpit and the feeder controller to establish communications and to verify descent clearance to 6000 ft MSL.

At the areas labeled Ⓓon the DRAKO approach and Ⓑ on the KEANN approach in figure 11, the TIMER generated a vector message and time at which the controller should initiate the corresponding turn command. This turn was to the downwind heading for the DRAKO approach and to a variable base-leg heading for the KEANN approach. The TIMER algorithm computed the heading compensation for wind to maintain the desired ground tracks. All requested headings were rounded to the nearest multiple of 10°. The next events were the handoff from the feeder controller to the final controller on the DRAKO approach (H) or a speed change to 170 knots

(S) immediately followed by the handoff (H) on the KEANN approach.

After communication was established with the cockpit, the final controller issued altitude clearances at his discretion to descend the subject aircraft to 1900 ft prior to intercepting the final-approach course. On the DRAKO approach, a speed adjustment (170 knots) was generated as the aircraft approached a specified location (S) on the downwind leg.

When approaching or when within the fine-tuning region, bounded by the dashed lines in figure 11, the direct-course error (DICE) with respect to the runway was periodically computed and displayed to the controller. As described in section 2.1, two DICE turns were generated for the DRAKO approach (B and F), and one DICE turn was generated for the KEANN approach (F). In conjunction with the last DICE turn, clearance was issued for the ILS runway 28L approach. As part of the instrument approach clearance, the pilot was instructed to contact the tower at the outer marker. For the remainder of the flight, the pilot continued on a normal ILS approach to the runway. Each run was flown to runway touchdown and terminated after starting the rollout.

3.2.3 Controller/Pseudo-Pilot Function

Arrival traffic inbound to the simulated Denver/Wallops Airport transits two terminal control sectors (the feeder sector and the final sector). The subject aircraft (the DC-9 simulator) was initialized in the feeder sector between 10 and 15 n.m. from the final control sector. Control instructions issued in this sector consisted of TIMER-generated commands that included turns off the initial inbound routing and speed reductions.

At the beginning of the run, the individual at ATC station 1 assumed the role of controller to the DC-9 simulator and other sector traffic; the individual at ATC station 2, a certified air traffic controller, acted as a pseudo pilot. As the aircraft entered the final sector, 3 to 4 minutes into the run, these roles were reversed for the duration of the run. Transfer of control to the final controller occurred after the subject aircraft received the initial turn off the inbound route (i.e., an easterly heading when on the DRAKO approach or a heading that varied between 150° and 200° for the KEANN approach). The transfer of communications occurred when the aircraft was instructed to "Contact Approach on 125.3," at which time the aircraft contacted the final sector.

In the final control sector, the aircraft was vectored to the final-approach course at the proper altitude using TIMER-generated fine-tuning commands

to reduce arrival-time error over the runway threshold. Aircraft were instructed to contact the tower at the outer marker; the controller then assumed the role of the tower controller and provided communications normally encountered by aircraft monitoring the tower frequency. To enhance realism, the landing clearance for the subject aircraft was issued at varying points along the final-approach course.

The procedures used for the ATC simulation were taken from the air traffic control manual (ref. 12) and were identical to those used in actual practice. The phraseology used and the clearances issued conformed both in content and format to those currently used in the real-world ATC system.

3.2.4 Controller Interface to TIMER

The TIMER-generated commands were presented as part of the alphanumeric data block associated with each aircraft. These data blocks were composed of 10 fields of text as described in figure 12. Fields 2 through 6 (shown shaded in fig. 12) contained information common to that found in terminal ARTS III data blocks. All other fields contain information that was unique to the TIMER program and not found in current ATC terminal data blocks. Field 1 was used to display the DICE value of aircraft in the fine-tuning region. The DICE value (described in section 2.2) decreased at a rate that was dependent on the ground track and speed of the aircraft. Field 7 displayed the TIMER-recommended heading and field 8 displayed the recommended airspeed. Fields 9 and 10 provided time-reference information with respect to the time at which the command should be delivered, the command delivery time (CDT).

For aircraft flying outside the fine-tuning region, the CDT's for speed and vector commands were computed using estimated ground speeds and tracks with respect to specified geographic locations. Thus, the required CDT's were generated well in advance of the aircraft reaching these locations. Within the fine-tuning region, however, the flight path geometry was somewhat variable. Therefore, the desired vectors for turning to the base and final-approach legs were not shown in the aircraft data tag until the actual clearance was generated, which was approximately 0 to 4 sec prior to the associated CDT.

The time remaining to the CDT provided useful information to the controller in integrating the issuance of the command into his workload. Should the command not be issued on time, a "countup" feature provided information needed to compensate for delinquency in delivery of the command. For example, if the program generated a left turn to 350° and the controller was 5 sec late in transmitting the

5

command, a turn to 340° might be issued instead if the controller judged that necessary for compensation.

The controller disabled the command by use of an electronic data tablet and an associated pen. The pen was moved upon the data tablet, which correspondingly moved a slaved "X" on the traffic display. When the "X" was placed over the appropriate data block and the pen switch depressed, the command and the time reference information were disabled. The data block then returned to its original state. The time at which the command and the time information were disabled was recorded and used to determine if the early or late delivery of a command might have influenced the arrival time of an aircraft at the runway threshold.

Figure 13 depicts the evolution of a data block that contains a vector control command. Figure 14 shows an example of a DICE countdown and ensuing vector command.

3.2.5 Subject Crew Profile and Experimental Task

Eight professional DC-9 rated pilots, four from each of two major U.S. airlines, served as test subjects for this study. Each pilot served as the captain and then the first officer for a crew, thus allowing eight full crews to be formed from the eight pilots. A crew was defined in the test matrix by the pilot serving as captain during the flights. The captain handled all flying duties during the flight, and the first officer handled communication and navigation radio functions, checklists, flaps, gear, etc. The individual subjects had experience in a variety of jet transport aircraft including the McDonnell Douglas DC-9 and DC-8; the Boeing 727, 737, and 757; the British Aerospace BAC 111; and the Lockheed L-1011 and C-141. The total jet transport experience ranged from a low of 4800 hours to a high of 13 300 hours, with an average of 6800 hours. The DC-9 experience ranged from a low of 1500 hours to a high of 6000 hours, with an average of 3500 hours.

The task presented to each crew was to fly either the KEANN route or the DRAKO route of the simulated Denver/Wallops Airport with a final approach and landing to runway 28L. The weather conditions simulated were those of Category I instrument flight rules with a ceiling of approximately 200 ft and a runway visual range of approximately 0.5 n.mi. Thus, the out-of-window visual scene presented an image of being in the clouds until the breakout occurred, at which point the crew would be able to see the runway and approach lights. The crew was requested to fly the aircraft as they normally would when using manual controls, manual throttles, and a flight

director. Figure 15 presents a simplified cockpit simulator procedure that occurred during the setup for each run and during each flight. The crew was to perform all normal flight-deck tasks associated with flying through a terminal area and making an approach and landing including normal checklists. (A normal checklist for each crew was that used by their particular airline.) The crew was requested to respond in a normal manner to air traffic control instructions for speed and altitude changes and vectoring maneuvers. As part of normal operations, the crew was required to accomplish all radio-communication frequency changes when instructed by air traffic control as the aircraft was handed off from sector to sector. Figures 16 and 17 present the navigation chart and ILS approach plate, respectively, used by the crews for this study.

3.2.6 Experimental Matrix and Parameters

The experimental organization or design is perhaps best shown in the following table:

Experimental condition	Simulation flights	Crew number		
		1	... n ...	8
Before TIMER Briefing	Practice	X	... X ...	X
	Run 1	X	... X ...	X
	Run 2	X	... X ...	X
	Run 3	X	... X ...	X
	Run 4	X	... X ...	X
After TIMER Briefing	Practice	X	... X ...	X
	Run 1	X	... X ...	X
	Run 2	X	... X ...	X
	Run 3	X	... X ...	X
	Run 4	X	... X ...	X
	Run 5		X	

A total of eight crews served as subjects in the TIMER/DC-9 experiment. A set of runs was made wherein each crew was requested to react to controller instructions as they normally would in instrument meteorological conditions (IMC) when transitioning to and executing an instrument approach. This series was called the "before-TIMER-briefing" runs. Each crew was given a full practice approach and then performed 4 data runs for a total of 32 before-briefing data runs.

Each crew was then briefed on the TIMER concept and how it was being applied, stressing that the performance depended on timely and consistent execution of ATC request. The presumption is that the after-briefing case represented pilots with a knowledge and awareness of the TIMER system, i.e.,

pilots who were motivated and attentive to ATC instructions. Another series of simulated approaches was flown. This second set of runs was labeled the "after-TIMER-briefing" runs. TIMER operation and controller procedures were consistent for both before- and after-briefing runs. Some crews performed 4 data runs and others performed 5 for a total of 37 after-briefing data runs. The following data were taken during the experiment:

Runway-threshold time error
Final-fix time error
DC-9 x,y,z position as a function of time
Pilot's response time to ATC turn instructions
DC-9 bank angle during turns
Captain's questionnaire rating
First officer's questionnaire rating
Controller's final-turn message-delivery-time error

In a human-in-the-loop experiment there is always the concern that the learning-curve phenomenon will have an effect that is falsely attributed to an experimental parameter. The following steps were taken to address this concern: (1) The DC-9 Full-Workload Simulator cockpit was utilized, (2) DC-9 certified, professional airline pilots were used as test subjects, (3) standard cockpit procedures were used during the flight, (4) no unusual or nonstandard items were in the cockpit such as experimental displays, and (5) the DC-9 simulator was developed with the technical guidance of a senior pilot from one of the two airlines providing pilots for this study. Also, before data were taken, each crew was briefed and given familiarization time in the DC-9 cockpit before performing a full-blown practice run. In addition, the performance data and crew questionnaire were cross-checked to determine if there was a progressive performance improvement due to a learning effect. Data from the crews' first data runs were compared with the fourth data runs within the before-briefing data set.

4.0 Real-Time Simulation Results and Discussion

Measurements were taken of the delivery-time precision achieved at the runway threshold and final-approach fix by a flight crew under realistically simulated full-workload conditions when flying a TIMER-assisted approach in a conventional electromechanical cockpit without a 4D FMS. Other real-time system performance parameters measured include final-approach speeds flown, approach routes and speeds flown, response time to controller's turn instructions, bank angles employed, and ATC controller's message-delivery-time errors. In addition,

aircraft-crew questionnaire data were collected after each simulated approach.

4.1 Piloted Simulation Performance

4.1.1 Delivery-Time Precision at Runway Threshold

The runway delivery-time precision achievable with conventional aircraft not equipped with a 4D FMS is a primary parameter of interest in this study. The cockpit/pilot airborne system performance was measured under crew-in-the-loop, realistic full-workload conditions. Figures 18 and 19 show the results before and after pilot briefing, respectively, of the cockpit simulator delivery-time errors at the runway threshold. The time errors are defined as the difference in threshold crossing times between the SLT and the recorded DC-9 simulator. It should be noted that the TIMER SLT's are dynamic, and thus the errors are relative to the last SLT used that occurs prior to the turn-to-final maneuver. Under the experimental conditions measured, the ATC controller's time error in delivering the final turn message, relative to the delivery time indicated by TIMER, was removed to isolate the combined TIMER system and pilot/cockpit simulator delivery precision.

In a crew-oriented experiment, there is always the concern that an effect attributed to an experimental parameter might, in fact, be caused by a learning-curve phenomenon. As mentioned earlier, several steps were taken to eliminate this effect. As a cross-check, the standard deviation of the DC-9 runway time errors for the first data run of each crew before briefing was computed and compared with the time errors of that crew's fourth data run before briefing. The standard deviation was 7.9 sec for the crews' first data run and 8.6 sec for the crews' fourth data run. Thus, there appears to be no progressive improvement in runway time-error standard deviation within the before-briefing data set that would indicate a learning effect.

The standard deviation of the DC-9 runway delivery-time error was computed for the runs both before and after pilot briefing. There are two significant and closely related issues here. One is whether there is a difference in the delivery precision before and after briefing. The other issue is the range of the delivery precision that can be expected with a TIMER-assisted approach to the runway.

With no time-error contribution by the ATC controller and with the assumption that the before-briefing case represents today's typical airline crew response, the data indicated a non-4D, single-aircraft, runway time-error standard deviation of 9.7 sec. The

experimental assumption was that the after-briefing case represented pilots with a knowledge and awareness of the system goals (i.e., pilots with attention and motivation to promptly and consistently respond to ATC instructions). The single-aircraft, runway time-error standard deviation computed for after-briefing runs was 7.0 sec.

The statistical F test was used to evaluate whether there was a difference in the standard deviation in before- and after-briefing runway time error. The null hypothesis for the F test contends that the ratio of the variance is 1 (i.e., $\sigma_{before} = \sigma_{after}$) at some significance α. For the before- and after-briefing standard deviations computed, the null hypothesis can be rejected at a significance of 5.6 percent. A confidence of 94.4 percent is slightly less conclusive than the desirable 95 percent; however, the statistical result does support the proposition that there was a small difference in the single-aircraft, runway time-error standard deviation before and after briefing. Though there appears to have been a slight reduction in the delivery precision after briefing, what is significant is how well the system works even with normal pilot response to ATC instructions. In fact, 7.0 to 9.7 sec can be treated as the range of single-aircraft standard deviations to be expected from airline pilots manually controlling an aircraft in response to verbal instructions from a final-approach controller who has computer aiding.

If Gaussian distributions are assumed, the total system (TIMER algorithms, pilot-in-the-loop, and controller) runway time-error variance for a single aircraft is

$$\sigma_d^2 = \sigma_p^2 + \sigma_c^2 \qquad (1)$$

where

σ_p pilot-in-the-loop/TIMER algorithm, time-error standard deviation for a single aircraft

σ_c standard deviation of controller's message-delivery-time error relative to TIMER expected delivery time

Assuming Gaussian distributions and a standard deviation of 2.3 sec in the ATC controller's message-delivery-time error (from section 4.2), the total system delivery-time-error standard deviation of single aircraft at the runway threshold would be 10.0 and 7.4 sec before and after briefing, respectively.

As described in reference 1, if Gaussian distributions are assumed, the relation between single-aircraft, runway time-error standard deviation and aircraft-pair, runway interarrival-time-error standard deviations is given by

$$\sigma_i = \sqrt{2}\,\sigma_d \qquad (2)$$

where

σ_d runway delivery-time-error standard deviation for a single aircraft

σ_i runway interarrival-time-error standard deviation for an aircraft pair

Using equation (2), the runway time-error standard deviations of 7.4 and 10.0 sec for single aircraft translate to interarrival-time-error standard deviations of 10.4 and 14.1 sec for corresponding aircraft pairs. These interarrival values bracket the 12 sec obtained in the earlier fast-time simulation and therefore support the reference 1 findings. As a point of reference, an FAA field study (ref. 2) measured a runway interarrival-time-error standard deviation of 26.5 sec for the aircraft pairs using manual control with no computer aiding. Thus, both the previous fast-time results and the real-time human-in-the-loop simulation results of this study show the potential of a time-based, terminal flow control system with controller aids such as those obtained in TIMER. With ground system knowledge of the aircraft final-approach speed, the runway interarrival-time-error standard deviation of the non-4D aircraft pair could be reduced to a region between 10.4 and 14.1 sec.

4.1.2 Delivery-Time Performance at Final-Approach Fix

Since the DC-9 simulator was configured with a known and constant landing weight for all the approaches, the pilot's flip-chart final-approach speed was also constant. The modeled and reported surface wind was also constant. Given these conditions, the time-error standard deviations at the final-approach fix (outer marker) should be in the proximity of those measured at the runway threshold. Figures 20 and 21 show the results before briefing the pilot and after briefing the pilot, respectively, of the time errors for the DC-9 simulator at the final-approach fix. The before-briefing standard deviations were 9.1 sec at the final-approach fix as compared with 9.7 sec at the runway threshold. The after-briefing standard deviations were 5.4 sec at the final-approach fix as compared with 7.6 sec at the runway threshold. The slightly higher standard deviations at the runway threshold relative to those at the final-approach fix, for both the before- and after-briefing cases, result from the variation in final-approach speeds flown by the individual pilots. The next section will address the final-approach-speed performance.

4.1.3 Final-Approach-Speed Performance

The final-approach speed is defined as the stabilized speed that the pilot reduces to on the glide slope when flying an instrument approach between

the final-approach fix and the runway. For each aircraft type there exists a final approach and landing speed (typically 1.3 times the stall speed) which, for the recommended flap setting, is a function of aircraft landing weight. The weight/speed information is typically contained in a tabular form in the pilot's takeoff- and landing-speeds flip chart. Generally, the recommended rule in airline training manuals is to add one-half the surface headwind plus the gust value to the indicated flip-chart speed. This resultant airspeed value will be referred to as the "expected final-approach speed." However, there is some variability in the wind adjustment from pilot to pilot.

Reference 1 showed that large variations from the expected final-approach speed would have a significant impact on runway interarrival error. Therefore, determining the extent of actual pilot variation in final-approach speed from that expected is an important parameter in assessing a terminal-area, time-based flow control system such as TIMER. The pilot's flip chart listed a final-approach speed of 130 knots for the DC-9 simulator-configured weight of 95 000 lb. Since the announced, simulated surface headwind was 8 knots, the resultant expected final-approach speed was 134 knots when using the above definition.

Figure 22 shows the mean and the spread of indicated airspeed along the entire final-approach course for all runs before briefing. The standard deviations of the cockpit-simulator indicated airspeed at the half-mile points are also shown. Figure 23 shows the same information for the runs after briefing. The airspeed magnitude and spread along the final-approach course are similar for both the before- and after-briefing runs. The average stabilized speed on final approach is approximately 139 knots, which is faster than the expected final-approach speed of 134 knots. The higher average speed would cause the individual aircraft to be slightly early relative to their scheduled landing time, but it would not affect the aircraft-pair interarrival-time error. The spread or standard deviation of final-approach speed from that expected does affect the aircraft-pair, runway interarrival-time-error standard deviation. The data of figures 22 and 23 show that the airspeed standard deviations were under 5 knots once the final-approach speed was established on the glide slope. The final-approach data, together with the following analysis at the ILS Category I window, provide a basis for modeling individual pilot variation in final-approach speed from that expected when performing ATC analysis of simulation modeling.

Figures 24 and 25 show the frequency distribution of the final-approach indicated airspeed sampled at

the ILS Category I window (about 200 ft above and 2800 ft horizontally from the threshold for a 3° glide slope) before and after briefing, respectively. The t and F tests even at a 20-percent level of significance indicated that both the means and the standard deviations of the final-approach speeds before and after briefing were not distinguishable. Consequently, the before and after final-approach speeds were combined to get the frequency distribution shown in figure 26. These pooled data indicated that the final-approach speed flown in the simulator was an average 4.8 knots faster than expected and the standard deviation was 3.7 knots. The 68 data approaches flown by the 8 pilots from 2 airlines support the premise that the data of figure 26 are representative of what can be expected from airline traffic under conditions similar to those simulated.

4.1.4 Approach Routes and Speeds Flown

Figure 27 shows the spatial distribution of the arrival-approach paths to the final-approach area flown by the crews in the data runs along with the nominal-approach paths. The aircraft positions are shown plotted every simulated radar scan of 4 sec. As discussed in section 3.1.1, the downwind and base legs are flown in response to heading and speed instructions from the ATC controller who, in turn, was interacting with the TIMER controller aids displayed on the PPI.

Figure 28 shows the base segment of all the KEANN data approaches (combined before- and after-briefing runs) with the darker position markers indicating aircraft locations every 10 scans or 40 sec. Figure 29 shows the corresponding aircraft indicated airspeeds and sample means with the sample standard deviations plotted for the corresponding 40-sec position points. The approach-path spreads and speed profiles between the before- and after-briefing runs did not differ significantly, and thus they were combined in a composite for the KEANN approach. In a similar manner, the before- and after-briefing runs were combined to show the approach-path spread and speed profiles of the DRAKO data approaches. These are shown in figures 30 and 31. The path divergence and airspeed data are presented so that ATC researchers may realistically model pilot performance in the terminal area.

Even though the wind model was not changed and each crew was given the same speed instruction for the same route, there was some variation in the speeds for both approaches flown. The airspeed standard deviation σ varied between 4 and 7 knots along the approaches. Data presented in figures 27 through 31 in the arrival-approach region and in

figures 22 and 23 along the final-approach region give a composite model of the aircraft pattern speeds as flown in the simulated environment.

4.1.5 Turn-Command Response Time of Aircrew

4.1.5.1 Turn-to-final-command response time of aircrew.

The timing of the turn-to-final maneuver from the base leg is the most crucial approach turn with respect to the aircraft arriving at the runway threshold at the scheduled landing time. Figures 32 and 33 show the histograms of pilot responses to ATC turn-to-final instructions before and after briefing, respectively. The pilot response time is defined as the elapsed time between hearing the ATC controller's turn instruction and the time when the aircraft is banked into the final turn $5°$ from the roll attitude at the time when the turn instruction was received in the cockpit.

The F test for differences of variance assumes Gaussian distributions. The data of figures 32 and 33 are somewhat skewed. Therefore, a data transformation of

$$t' = 0.734(t - 0.9)^{0.55} + 4.137 \qquad (3)$$

was used (ref. 13) on each data point to approximate a Gaussian distribution. The F test on the transformed response-time data before and after briefing yielded an F statistic of

$$F = \frac{(0.6)^2}{(0.5)^2} = 1.44 \qquad (4)$$

Even at the 20-percent level of significance, the transformed, turn-to-final response-time standard deviation after briefing could not be considered different from the standard deviation before briefing. The pilots' mean response times before and after briefing were equal for both the measured data and the transformed data. Therefore, the means of the pilots' response times as well as the standard deviations before and after briefing should be considered equal.

4.1.5.2 Turn-to-final-command response-time model of aircrew.

Since there was no significant statistical difference at the base-to-final turn between the pilot response times before and after briefing, they were combined as shown in figure 34. A three-parameter Weibull distribution with probability density function

$$
\left.
\begin{aligned}
f(t) &= \frac{\beta}{\eta}\left(\frac{t-\gamma}{\eta}\right)^{\beta-1} \exp\left[-\frac{(t-\gamma)^\beta}{\eta}\right] && (t \geq \gamma;\ \eta, \beta > 0) \\
f(t) &= 0 && (t < \gamma)
\end{aligned}
\right\} \qquad (5)
$$

was fitted to the combined response-time data for the base-to-final turn. A threshold of 0.9 was selected and the mean and variance of the Weibull distribution were set equal to the measured combined data in order to solve for the parameters η and β. This yielded values of $\gamma = 0.9$, $\beta = 1.1$, and $\eta = 2.28$. The resultant fitted Weibull density function is superimposed on the measured data in figure 34. Reference 14 provides justification for using a Weibull distribution to model the human response time. Thus, we have an analytical expression for the probability density function of the pilot's response time to the ATC controller's turn-to-final instruction. The cumulative distribution of the three-parameter Weibull distribution is equal to

$$
\left.
\begin{aligned}
F(t) &= 1 - \exp\left[-\frac{(t-\gamma)^\beta}{\eta}\right] && (t \geq \gamma;\ \eta, \beta > 0) \\
F(t) &= 0 && (t < \gamma)
\end{aligned}
\right\} \qquad (6)
$$

The histogram and fitted-density model of figure 34 are the delay responses of 8 airline pilots performing 62 turn-to-final maneuvers. The model represents a simple input/output relationship and does not address the detailed contributing factors. There are several possible explanations such as variations in individual pilot routine response to ATC turn instruction, pilot workload or cockpit activity at the time that the turn instructions were issued, and differences in piloting procedures when initiating a turn. For example, initiating the turn before setting the "bug" on the directional gyro display would produce a different response time from the procedure of setting the bug and then initiating the turn. Another controlled and more focused experiment would be required to identify and isolate contributing factors. Such an experiment could determine if training would change the crew's response-time curve.

4.1.5.3 Approach-turn-command response time of aircrew.

Figures 35 and 36 show the pilot response times to controller turn instructions both before and after briefing, respectively, at the first turn on the KEANN approach route (Ⓔ in fig. 11(b)). Correspondingly, figures 37 and 38 show the response-time data before and after briefing for the first turn on the DRAKO approach (Ⓓ in fig. 11(a)). Similarly, figures 39 and 40 show the response-time data before and after briefing for the second or downwind-to-base turn on the DRAKO approach (Ⓑ in fig. 11(a)).

For each of these earlier turns, rigorous statistical tests on these data are not very enlightening because of the limited sample sizes. No statistical differences in the pilot response times before and after briefing at each of these earlier turns can be claimed. For

the same reason, no response-time difference among the turns themselves can be rigorously substantiated. However, there are a couple of observations about the trends in the plotted data that are worth noting. One is that the response-time scatter for these earlier turns in the approach before briefing seems to be somewhat reduced after briefing. The other observation is that the closer the aircraft gets to the runway the more the response-time data tend to get skewed with a larger percentage of the reactions concentrated at smaller response times.

4.1.6 Bank-Angle Performance

For each of the controller-issued turns during the approach, the value of the maximum bank angle was recorded because bank angle has an effect on time error at the runway. A variation in the bank angle will vary the radius of the turn and, thus, the distance traveled and the time of arrival. A time error will result if the pilot uses a bank angle that is significantly different from that assumed in the TIMER algorithm. The bank angles flown by the test crews during the turn-to-final maneuver from the base leg are examined first and in greater detail than the other turns since that turn is the most crucial relative to runway-arrival time accuracy. Figures 41 and 42 show the histograms of maximum bank angles used in the turn-to-final maneuver before and after briefing, respectively.

There are two noteworthy differences between the before- and after-briefing bank-angle distributions for the turn-to-final maneuver. The bank-angle density is considerably skewed before briefing but is more symmetrical after briefing. The other difference observed is that the bank angles after briefing are more closely bunched. The standard deviation, which measures dispersion, is 2.8° after briefing as compared with 4.6° before briefing. The F test at the 0.7-percent significance strongly supports the hypothesis that the subject pilots kept their bank angles in a narrower range of values after the briefing while performing the base-to-final turn.

A Weibull distribution, with the probability density function defined by equation (5), was fitted to the data of figures 41 and 42. The parameters of the Weibull distribution before briefing are $\gamma = 19$, $\beta = 1.51$, and $\eta = 7.54$. The parameters of the Weibull distribution after briefing are $\gamma = 20$, $\beta = 2.56$, and $\eta = 7.55$. The fitted curves for before and after briefing are shown in figures 41 and 42, respectively. These distributions can be used to model individual pilot variation in the selection of bank angle for the base-to-final turn.

Figures 43 and 44 show the maximum bank angle employed when turning to the base leg on the

KEANN approach (Ⓑ in fig. 11(b)) both before and after briefing, respectively. The bank-angle standard deviations computed were 5.0° before briefing and 3.2° after briefing. For the values computed before and after briefing, the significance must be at least 8 percent in order to reject the null hypothesis (i.e., $\sigma_{before} = \sigma_{after}$). Because of the limited sample size, there is a less-than-conclusive statistical case for the contention that there was a difference in the bank-angle standard deviations before and after briefing for the turn-to-base maneuver on the KEANN approach.

Figures 45 and 46 show the maximum-bank-angle data before and after briefing, respectively, for the turn to the downwind on the DRAKO approach (Ⓓ in fig. 11(a)). The standard deviation was only slightly reduced from 3.8° to 3.2°. There was no statistical significance to the bank-angle standard deviations before and after briefing on the turn-to-downwind maneuver on the DRAKO approach.

Figures 47 and 48 show the maximum-bank-angle data before and after briefing for the turn-to-base leg on the DRAKO approach (Ⓑ in fig. 11(a)). The bank-angle standard deviations computed were 3.4° before briefing and 2.2° after briefing. For the values computed before and after briefing, the significance must be at least 9 percent in order to reject the null hypothesis of equal variances. Because of the limited sample size there is a less-than-conclusive statistical case for the contention that there was a difference in the bank-angle standard deviations before and after briefing for the turn-to-base leg on the DRAKO approach.

The rigorous statistical test on the earlier terminal approach turns before the base-to-final turn was not as conclusive as would have been desired because of the limited sample sizes. However, the trends in the plotted data shown in figures 43 through 48 for these three earlier turns all seem to indicate the scatter of the maximum bank angle before briefing was reduced somewhat after briefing. There were no significant differences between the before- and after-briefing performances observed for the other aircraft parameters measured such as speed and time responses. However, the maximum bank angle was an exception. The tendency to reduce the dispersion or spread of the bank angle after the pilots received the TIMER briefing was clearly evident in the data on the base-to-final turn. The reduction in the standard deviation of the bank angles measured after briefing for the base-to-final turn was apparently enough to translate to a slight, though statistically significant (at the 5.6-percent level), impact on the delivery-time performance at the runway threshold.

11

4.1.7 Final-Approach Data

To characterize and gather data for modeling of crew and airborne system performance during the final stages of the flight, various data such as altitude, vertical tracking of the glide slope beam, lateral tracking of the localizer beam, and airspeed were monitored and recorded continuously. In addition, snapshot data were recorded at the ILS Category I window and the runway-threshold window. Little or no difference was seen between crews, between airlines, or between before and after briefing; therefore, only mean and standard deviation plots of all runs before briefing are presented for the final-approach parameters. For the snapshot data, all data for all runs are presented on single plots.

Figure 49 presents the mean and standard deviation plots for all runs/all crews for flights conducted before briefing. Altitude performance, localizer tracking, airspeed performance, and rate-of-descent performance are plotted versus distance from the runway threshold. The plots begin just before intercept of the glide slope beam. The data for the flights after briefing are very similar to those presented herein.

Figure 50 presents snapshot data for the glide slope error and localizer error for the Category I window. The ILS Category I window was 200 ft above the ground where the crew must acquire the runway environment in order to land. The data presented are for all crews and all runs both before and after briefing. All runs were within acceptable parameters and were completed to touchdown. Figure 51 presents the same data at the runway-threshold window.

4.1.8 Crew Questionnaire and Results

In addition to recording the physical data described above, a rating sheet was administered to the captain and first officer at the end of each flight. The major objectives of the rating sheets were (1) to determine if, after briefing, crew concern about prompt and consistent response to ATC request raised their perceived workload, and (2) to establish whether the simulation was realistic and representative of real-world conditions.

The rating sheet contained eleven 7-point scales featuring bipolar adjective pairs that dichotomized the following descriptors: (1) physical workload (low/high), (2) cognitive workload (low/high), (3) perceptual workload (low/high), (4) overall workload (low/high), (5) safety (safe/not safe), (6) passenger acceptance (acceptable/not acceptable), (7) skill required (minimum/maximum piloting skill), (8) controllability (easy to control/hard to control), (9) uneasiness (not uneasy/uneasy), (10) crew members' performance (satisfactory/unsatisfactory), and

(11) ATC assessment (identical/very different). In addition, space was provided for any additional comments that the crew members desired to make about the flight. Figure 52 presents an example of the rating sheet. A list of rating sheet definitions (fig. 53) was presented to each crew member before the flight began, and this definitions list was available to the crew as they filled out the rating sheet after each flight. This rating sheet has been developed over several studies and was used in its present form with a high degree of success in the study discussed in references 15 and 16.

The ratings selected by each crew member from the 7-point scale were converted to a number in the range of 1 to 7 for each subjective descriptor, where a "1" represented the most favorable rating (the lowest workload, etc.) and a "7" represented the least favorable rating (the highest workload, etc.). Average ratings across all captains and the corresponding standard deviations were then computed for each of the subjective descriptors on the rating sheet. This was done both for the flights conducted before briefing and for the flights conducted after briefing. The same data reduction process was performed for the first officers.

In order to ensure that differences seen in the data between before briefing and after briefing were due to the briefing and not due to training effects, the data were tested for training effects using a statistical t test. The first flight before briefing for all crews was compared with the last flight before briefing for all crews. No statistically significant difference was detected for any of the descriptors between the first flight and the last flight, thus indicating that there were no training effects present in the data.

For the captains, each workload category (fig. 54) was rated on the favorable end of the scale for the flights before briefing and improved slightly after the briefing. A significant difference was detected at the 5-percent level between before briefing and after briefing for physical workload and perceptual workload. The first officers' workload ratings for runs both before and after briefing indicate less workload than the captains' ratings. Although the first officers' results showed a slight reduction in their workload ratings after briefing, the differences were not statistically significant. The important point is that the crews' after-briefing awareness of the importance of attention and prompt response to the ATC request did not raise the perceived workload and, if anything, the challenge may have even lowered their subjective perceived workload.

For the next six categories rated by the captains (fig. 54), all categories were rated in the most favorable one-third of the scale with only "skill required"

and "crew member performance" rated above 2.3 before briefing. After briefing, all six categories improved with only "skill required" rated above 1.9. Although a significant difference between before briefing and after briefing was detected at the 5-percent level for "controllability" and "uneasiness," and at the 1-percent level for "crew member performance," it should be emphasized that all ratings were in the most favorable section of the scale. Bear in mind that the ratings are subjective, and thus the general range on the scale is more important than the absolute value. For the first officers (fig. 55), little difference was seen in the ratings between before and after briefing, and no significant differences were detected. Except for "skill required" (which was rated at 2.7), the other five categories were rated between 1 and 2. There are two significant points to be made from the six rating categories discussed above as well as from pilot comments. The crews indicated that the maneuvers were nominal and would cause no passenger acceptance problems. In the crews' judgment, no unusual pilot skill would be required to perform the TIMER-assisted approaches.

The final category to be rated was that of "ATC assessment," where an attempt was made to see if the crew members perceived any significant differences between the simulated ATC environment and the real world. As can be seen from the figures, the crew members rated the simulated environment virtually identical to the real world.

4.2 ATC Controller's Message-Delivery Performance

Since the TAATM simulation was originally designed to provide a realistic environment for cockpit research, pseudo-pilot capability to drive all simulated aircraft was not available at the time of this experiment. Lack of pseudo-pilot aircraft control capability was acceptable because the primary focus of the experiment was to measure the performance of conventional aircraft (without a 4D flight management system) in a TIMER environment. Consequently, the pilots in the cockpit simulation reacted to the controller's verbal command; however, the other simulated aircraft were under the control of the TIMER real-time program. As discussed in section 3 and shown in figure 7, the verbal commands to the other traffic were issued to a pseudo pilot who verbally replied and initiated radio contact, but did not actually input trajectory commands.

Figure 56 shows the delivery errors (relative to the TIMER expected delivery times discussed in sections 2.2 and 3.2.4) of the ATC controller's final-turn instruction to the DC-9 cockpit. The timing information obtained depended on the controller

manually activating an electronic data tablet immediately after message delivery to halt a computer timer that was activated by the DICE countdown. There was some human time inaccuracy in activating the data tablet relative to message delivery, which contributed some imprecision to the controller's measured time errors in message delivery. However, the plotted values of figure 56 are a reasonable estimate of the time errors by the controller in delivering the final-turn instruction to the DC-9 cockpit. The measured delivery errors had a mean of 1.0 sec late and a standard deviation of 2.1 sec. A three-parameter Weibull distribution with a density given by equation (5) was fitted to the data as shown in figure 56. The parameters of the plotted Weibull distribution are $\gamma = -4.0$, $\beta = 2.52$, and $\eta = 5.63$.

Figure 57 shows the controller's measured time errors in delivering the final-turn instruction to the TIMER simulated traffic other than the DC-9 cockpit. The measured delivery error had a mean of 1.8 sec late and a standard deviation of 2.7 sec. A three-parameter Weibull distribution with a density given by equation (5) was fitted to the data and is also shown in figure 57. The parameters of the plotted curve are $\gamma = -4.0$, $\beta = 2.25$, and $\eta = 6.54$.

The ATC controller was an integral part of the TIMER/DC-9 experiment. Therefore, he knew that commands issued to other TIMER simulated and controlled aircraft, although adding realism to the DC-9 cockpit environment, did not affect the trajectory of that other traffic. Given this situation, the subject controller could have inadvertently paid more attention to issuing instructions to the DC-9 cockpit than would have been the case if all the traffic depended on his instructions. The data of figures 56 and 57 support that hypothesis. The delivery-time-error standard deviation of the controller's final-turn instruction to the DC-9 cockpit (2.1 sec) was compared with the standard deviation to the TIMER internally controlled traffic (2.7 sec). The standard F test indicated that at the 2-percent level of significance, there was a difference between the two standard deviations.

It is reasonable to assume that the subject controller's final-turn message-delivery performance in an operational TIMER environment is bounded by the two cases shown in figures 56 and 57. A standard deviation of 2.3 sec was used in section 4.1 to compute the system interarrival-error performance. Although showing the performance of only one controller, the data represent a credible initial estimate of general controller performance. A more rigorous experiment to characterize the controller's performance of message delivery-time-error performance of controllers in general in an operational TIMER-like

environment would require two additional conditions: (1) the trajectory of all simulated aircraft dependent upon controller instruction, and (2) the measurement of a number of certified and practicing final-approach controllers as subjects.

4.3 Potential TIMER Improvements

Sections 2 and 3 described the TIMER concept and the mode of controller interface used for this study. Experience with the reported real-time study and discussions with the experimental subjects have led to some ideas that have the potential for improving performance and acceptance.

4.3.1 Procedural Changes

The calculations used by TIMER during the experiment assume that the pilots follow a procedure in which they deploy the landing gear after interception of the lower edge of the glide slope, then fully deploy the landing flaps. The resultant speed profile is a pattern of deceleration across the final-approach fix (outer marker) from approach speed to final as shown in figures 22 and 23. There is some variation in the point where speed reduction begins because of altitude and piloting procedure. An alternative procedure often used in ATC practice, particularly at the busier terminals, is for the controllers to request that aircraft maintain speed to the final-approach fix. This procedure has the potential of slightly reducing the variation of the location where transition from approach to final speed begins, thus making the time duration along the final path slightly more consistent.

Headings in the real-time test were given to the nearest 10°. A resolution of the heading value to the nearest 5° was suggested since that is sometimes used in practice. It is true that 5° resolutions would better match the aircraft path with the desired ground track. However, based on the fast-time sensitivity study of reference 1, a reduction of less than 1 sec in the interarrival-error standard deviation would be expected from flying headings to the nearest 5°. The extent of pilot compliance with more precise heading instructions is not known; however, subject reaction to the proposal indicated no pilot reluctance to flying headings with a 5° resolution.

4.3.2 Controller's Interface Alternatives

The current TIMER approach is to transmit the suggested commands to the controller via the aircraft data tags by adding more fields of information to that currently displayed by the ARTS system. The authors feel that is the location of choice because it is in the normal field of view where the controller's attention can remain focused on the aircraft locations and proximity to other aircraft. In addition, when

action is called for, the particular aircraft involved is readily apparent since its data tag contains the information. However, there is another point of view which holds that the ARTS data tags already contain enough information. In addition to possible information saturation, the additional fields in the data block would magnify tag offset from the aircraft symbol in congested conditions. Another approach to be explored is to have TIMER suggested commands appear in a special position on the PPI screen or in a message window. In this format, the messages would probably be ordered on their desired delivery times.

In the real-time experiment the DICE procedure was implemented by displaying the new desired heading only after the DICE countdown reached zero. The reason is that the calculated desired heading occasionally changes as a function of wind profile, aircraft altitude, schedule change, and projected runway-centerline intercept distance from the final-approach fix. An alternative procedure would be to display the projected heading earlier even if some error resulted. This trade-off needs further controller evaluations to determine if earlier heading display improves performance or reduces controller workload.

Another idea that has potential application in TIMER command/controller interaction also has broader potential applications. Borrowing from the military concept of look-to-aim weapons in aircraft, an idea was advanced to use an automatic cursor that follows controller lookpoint. This technique could potentially be quicker and less tiring than a trackball or even a touchscreen. Instruments such as the occulometer (ref. 17) could be used as a basis to explore this technique.

5.0 Major Results and Concluding Remarks

Several facilities including a full-workload DC-9 cockpit and a real-time TIMER (traffic intelligence for the management of efficient runway) simulation were coupled together. These facilities together with a certified air traffic control (ATC) controller, pseudo pilot, and airline crew formed the basis of a total system simulation for real-time crew-in-the-loop experiments. Performance data were gathered as the crew flew simulated instrument flight rules (IFR) approaches with a Denver Stapleton runway 26L configuration. The following is a summary of the major findings.

Based on the measured real-time cockpit delivery error at the runway threshold, a system aircraft-pair interarrival-error standard deviation was determined to be in the range of 10.4 to 14.1 sec. The 14.1 sec results from measurements taken when DC-9 certified

airline pilots were asked to fly manual approaches as normally done in their company DC-9 aircraft. The 10.4 sec results from measurements taken after the pilots were briefed on the TIMER concept and how its performance depended on timely and consistent execution of ATC request. The aircraft-pair, runway interarrival-error standard deviation ranging from 10.4 to 14.1 sec supported the 12 sec predicted by earlier TIMER fast-time simulations.

There was a slight improvement in the delivery performance after the crew briefing. Presumably, the after-briefing situation represented pilots with knowledge and awareness of the importance of airborne crew performance, i.e., pilots that were motivated and attentive. What is significant about these results is how well the TIMER system worked even with normal pilot response to ATC instructions. As a point of reference, a field study by Martin and Willett in 1968 measured 26.5 sec as the aircraft-pair, runway interarrival-error standard deviation of manual control with no computer aiding. The real-time, human-in-the-loop simulation results of this study, as well as earlier fast-time results, show the potential of a time-based, terminal-area flow control system with controller aids such as those obtained in TIMER. With ground knowledge of the aircraft final-approach speed, the non-four-dimensional (non-4D), runway interarrival-error standard deviation of an aircraft pair could be reduced to a region between 10.4 and 14.1 sec.

The extent of pilot-induced variation in final-approach speed from that expected for an aircraft type and landing weight is an important parameter in assessing a terminal time-based flow control system such as TIMER. The means and standard deviations of the final-approach speeds before and after briefing were not distinguishable. The pilot-induced variation in the final-approach speed flown in the simulator was an average 4.8 knots faster than expected, and the standard deviation was 3.7 knots. These data are significant because of the current limited data base for the modeling of pilot/aircraft performance in the field of ATC system analysis and simulation modeling.

The measured pilot response times to the turn-to-final instruction before and after briefing were not distinguishable. The before- and after-briefing data were pooled and fitted with a three-parameter Weibull distribution. Thus, an analytical expression was obtained for the probability density and the cumulative distribution of pilot response time to the ATC controller's turn-to-final instruction. This model should be used in ATC system analysis and simulation modeling rather than a Gaussian distribution because of the considerable skewness of the pilot's response times.

There are two noteworthy differences between the before- and after-briefing bank angles used by the pilots during their turn-to-final maneuver. The bank-angle density is considerably skewed before briefing, but the after-briefing density is almost symmetrical. The other difference is that of scatter—the bank-angle standard deviation was 4.6° before briefing and reduced to 2.8° after briefing. The reduced scatter of the bank-angle values after briefing was apparently the reason for the slight improvement in delivery precision measured after crew briefing. A distribution was fitted to the bank-angle data that can be used for analysis and computer simulation.

There are a few points worth mentioning about results from the questionnaire administered to both the captain and first officer after each simulated flight. The crews felt strongly that the ATC instructions and simulation scenarios, both before and after briefing, were representative and close to realistic real-world conditions. The crews' after-briefing awareness of the importance (relative to precise runway-threshold delivery time) of attention and prompt response to an ATC request did not raise their perceived workload, and, if anything, the challenge may have even lowered the crews' subjective perceived workload. The crews indicated that the maneuvers were nominal and would cause no passenger acceptance problems. In the crews' judgment, no unusual pilot skill would be required to perform the TIMER-assisted approaches.

Because of the nature of the simulation, only the DC-9 cockpit reacted to the controller's verbal commands. The other traffic was under internal TIMER control. Thus, the controller's time errors (relative to the TIMER expected time) in delivering the final-turn instruction were separated into errors to the DC-9 cockpit and errors to the other TIMER traffic. A three-parameter Weibull distribution was fitted to these two data sets. The controller's message delivery-time error to the DC-9 cockpit had a mean of 1.0 sec late and a standard deviation of 2.1 sec. The controller's time error to the internally controlled TIMER aircraft had a mean of 1.8 sec late and a standard deviation of 2.7 sec. If all the traffic had been controlled by responding live crews, it is felt that the controller's performance would lie between the two measured cases above.

References

1. Credeur, Leonard; and Capron, William R.: *Simulation Evaluation of TIMER, a Time-Based, Terminal Air Traffic, Flow-Management Concept.* NASA TP-2870, 1989.

2. Martin, Donald A.; and Willett, Francis M., Jr.: *Development and Application of a Terminal Spacing System.* Rep. No. NA-68-25 (RD-68-16), Federal Aviation Adm., Aug. 1968.

3. Credeur, Leonard; Davis, Christina M.; and Capron, William R.: *Evaluation of Microwave Landing System (MLS) Effect on the Delivery Performance of a Fixed-Path Metering and Spacing System.* NASA TP-1844, 1981.

4. Andrews, John W.; and Welch, Jerry D.: The Challenge of Terminal Air Traffic Control Automation. *34th Annual Air Traffic Control Association Conference Proceedings— Fall 1989,* Air Traffic Control Assoc., Inc., c.1989, pp. 226–232.

5. Davis, Thomas J.; Erzberger, Heinz; and Bergeron, Hugh: *Design of a Final Approach Spacing Tool for TRACON Air Traffic Control.* NASA TM-102229, 1989.

6. Davis, Thomas J.; and Green, Steven M.: *Piloted Simulation of a Ground-Based Time-Control Concept for Air Traffic Control.* NASA TM-101086, 1989.

7. Erzberger, Heinz; and Nedell, William: *Design of Automation Tools for Management of Descent Traffic.* NASA TM-101078, 1988.

8. Benoît, André; Swierstra, Sip; and De Wispelaere, René: Next Generation of Control Techniques in Advanced TMA. *Efficient Conduct of Individual Flights and Air Traffic or Optimum Utilization of Modern Technology for the Overall Benefit of Civil and Military Airspace Users,* AGARD-CP-410, Dec. 1986, pp. 55E-1–55E-15.

9. Völckers, U.: Computer Assisted Arrival Sequencing and Scheduling With the COMPAS System. *Efficient Conduct of Individual Flights and Air Traffic or Optimum Utilization of Modern Technology for the Overall Benefit of Civil and Military Airspace Users,* AGARD-CP-410, Dec. 1986, pp. 54-1–54-11.

10. Kaylor, Jack T.; Simmons, Harold I.; Naftel, Patricia B.; Houck, Jacob A.; and Grove, Randall D.: *The Mission Oriented Terminal Area Simulation Facility.* NASA TM-87621, 1985.

11. Rollins, John D.: *Description and Performance of the Langley Visual Landing Display System.* NASA TM-78742, 1978.

12. *Air Traffic Control.* 7110.65E, Federal Aviation Adm., Apr. 9, 1987.

13. Wall, Francis J.: *Statistical Data Analysis Handbook.* McGraw-Hill, Inc., c.1986.

14. Berry, Gayle L.: The Weibull Distribution as a Human Performance Descriptor. *IEEE Trans. Syst., Man, & Cybern.,* vol. SMC-11, no. 7, July 1981, pp. 501–504.

15. DeLoach, Richard; and Houck, Jacob A.: Pilot Evaluation of Experimental Flight Trajectories in the Near-Terminal Area. *A Collection of Technical Papers—AIAA Atmospheric Flight Mechanics Conference,* Aug. 1986, pp. 97–110. (Available as AIAA-86-2074.)

16. DeLoach, Richard; and Houck, Jacob A.: Pilot Evaluation of Population—Minimal Ground Tracks in the Airport Community. *J. Aircr.,* vol. 24, no. 9, Sept. 1987, pp. 603–610.

17. Harris, Randall L., Sr.; Glover, Bobby J.; and Spady, Amos A., Jr. (appendix A by Daniel W. Burdette): *Analytical Techniques of Pilot Scanning Behavior and Their Application.* NASA TP-2525, 1986.
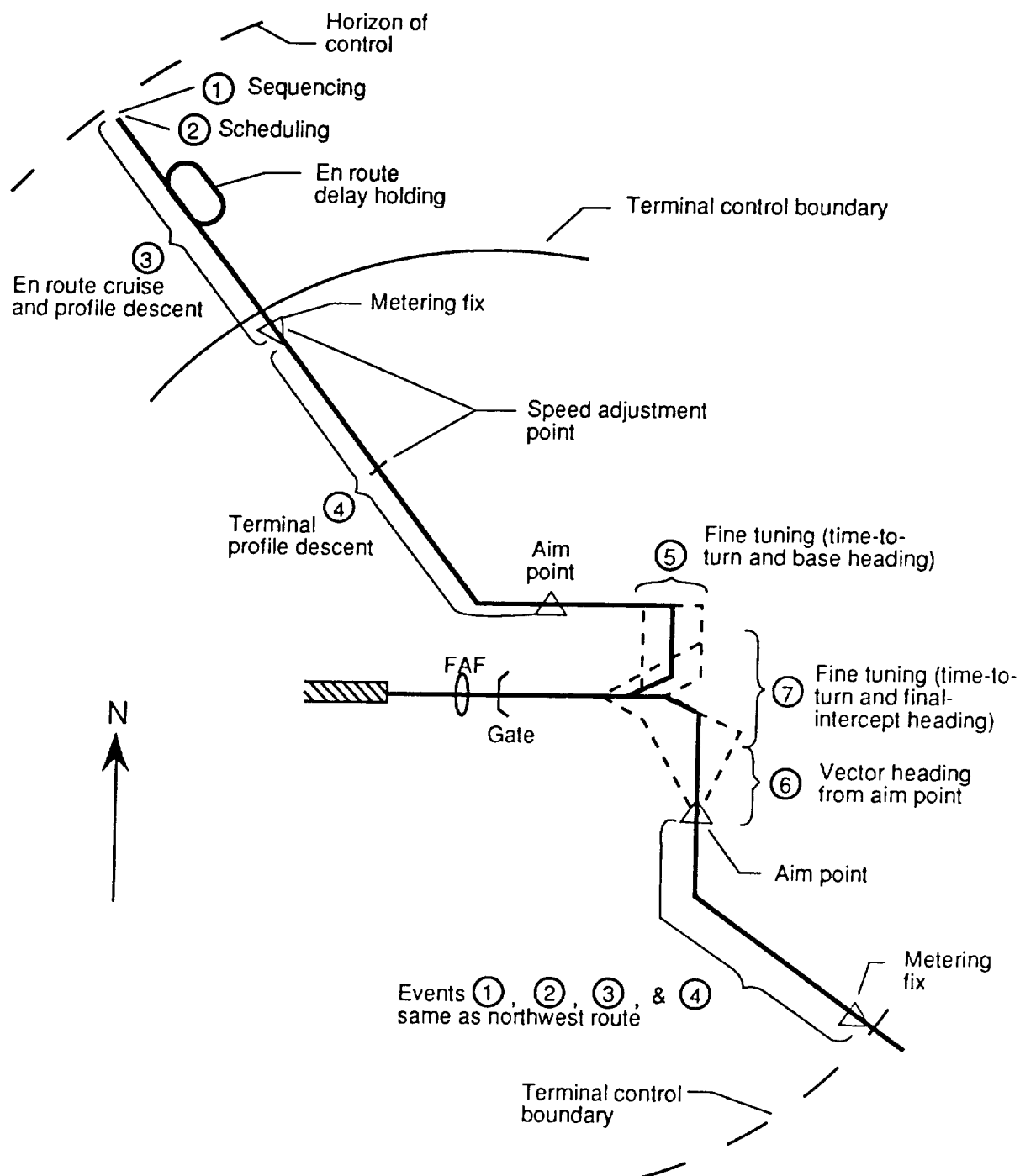
Figure 1. Sequence of events that an arrival aircraft would experience in TIMER concept.
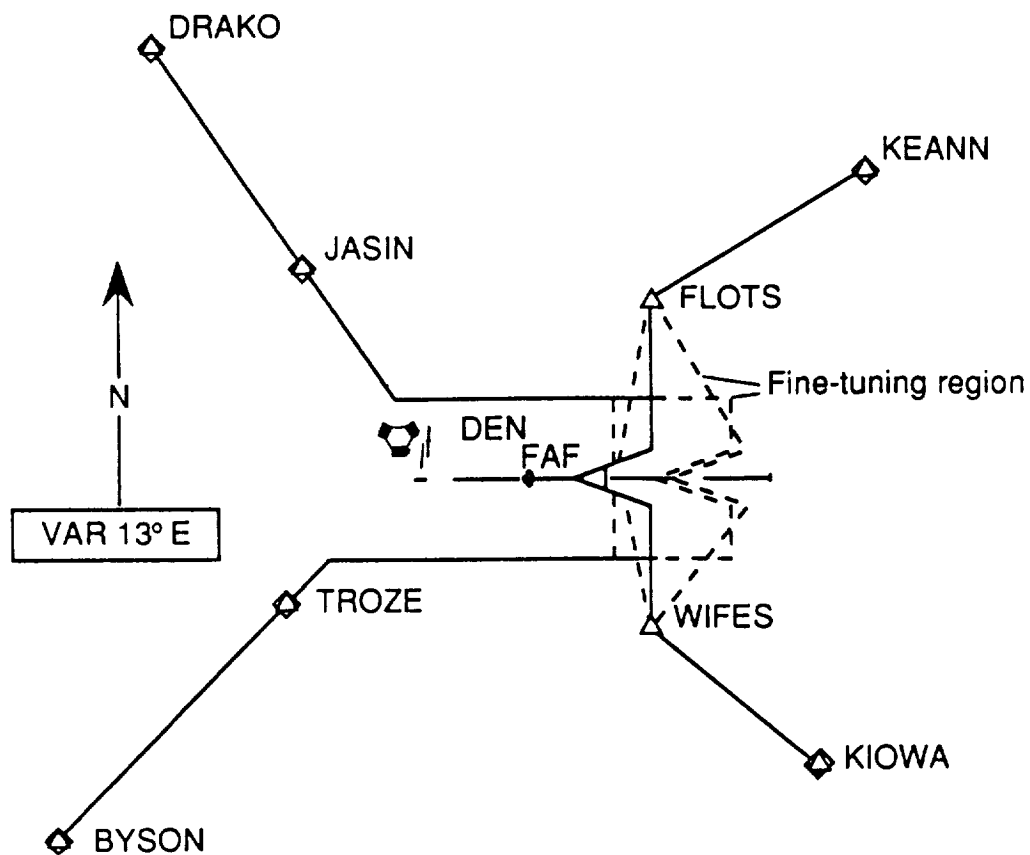
Figure 2. Terminal geometry simulated for approaches to runway 26L at Denver's Stapleton International Airport.

DC-9 Simulator

Wallops Flight Facility

L-88-9499

ATC controller station
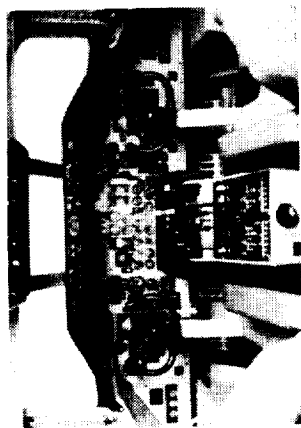
Terminal-area model
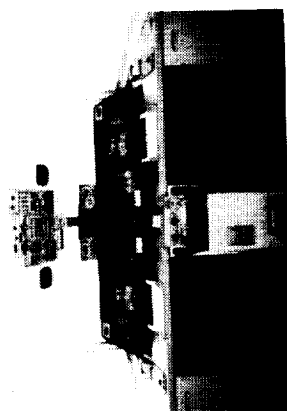
Advanced Concepts Simulator
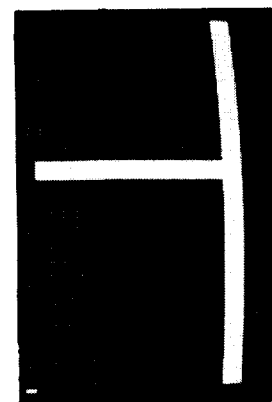
TSRV Simulator

Pseudo-pilot station

Figure 3. The Mission-Oriented Terminal-Area Simulation (MOTAS) Facility.

19
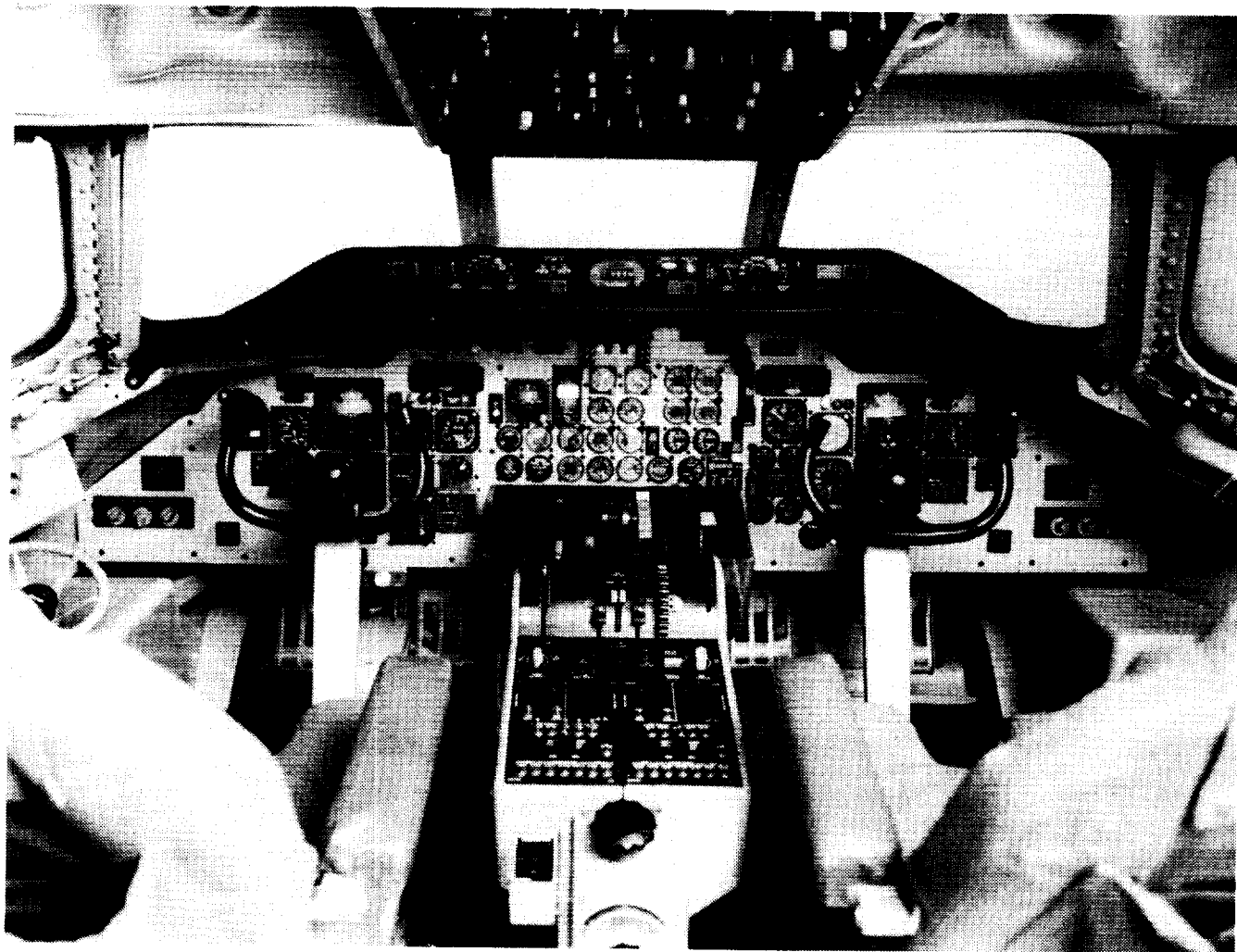
L-82-10572

Figure 4. The DC-9 Simulator.

L-75-7494

Figure 5. The Visual Landing Display Simulator.
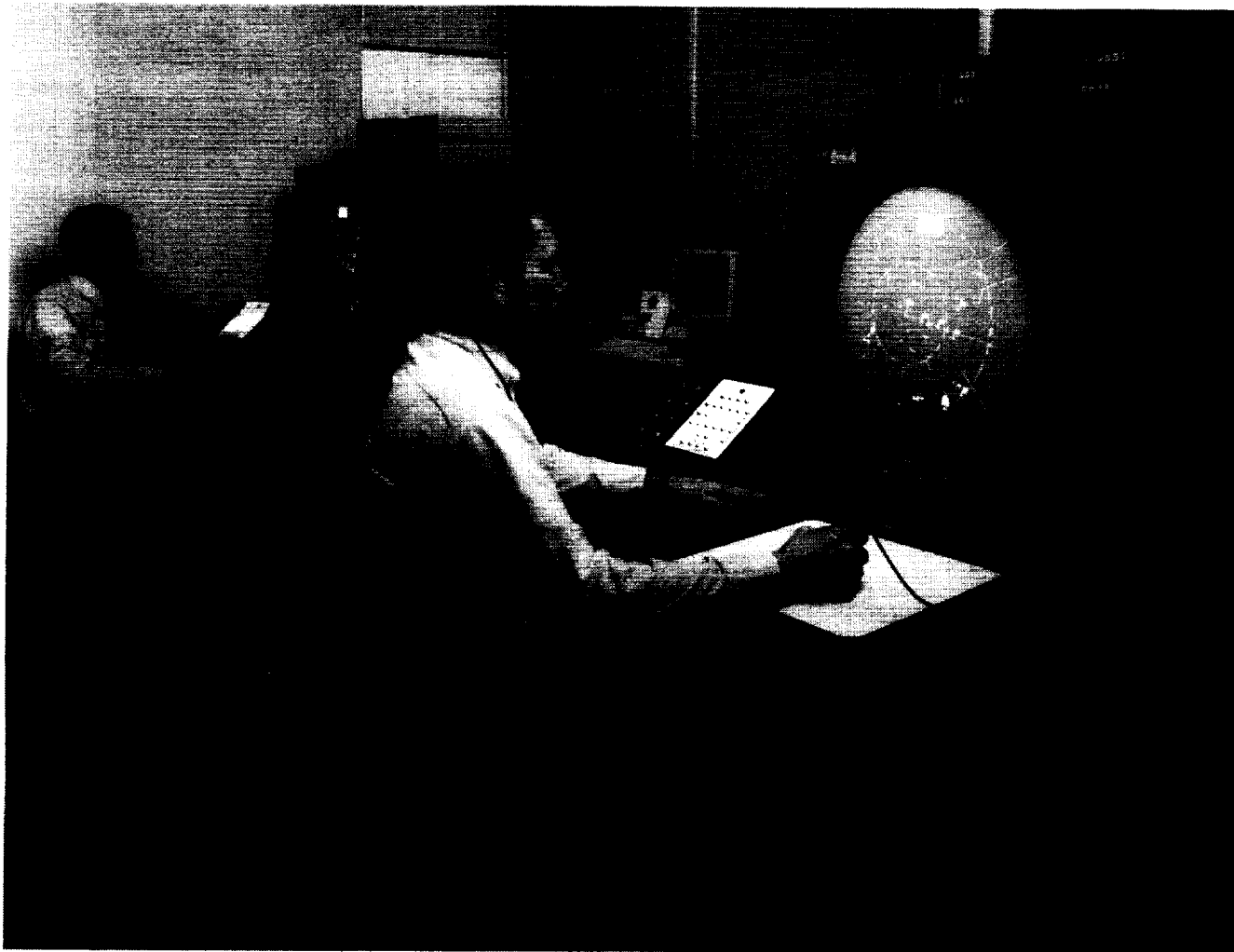
L-89-2574

Figure 6. Simulation air traffic controller stations.
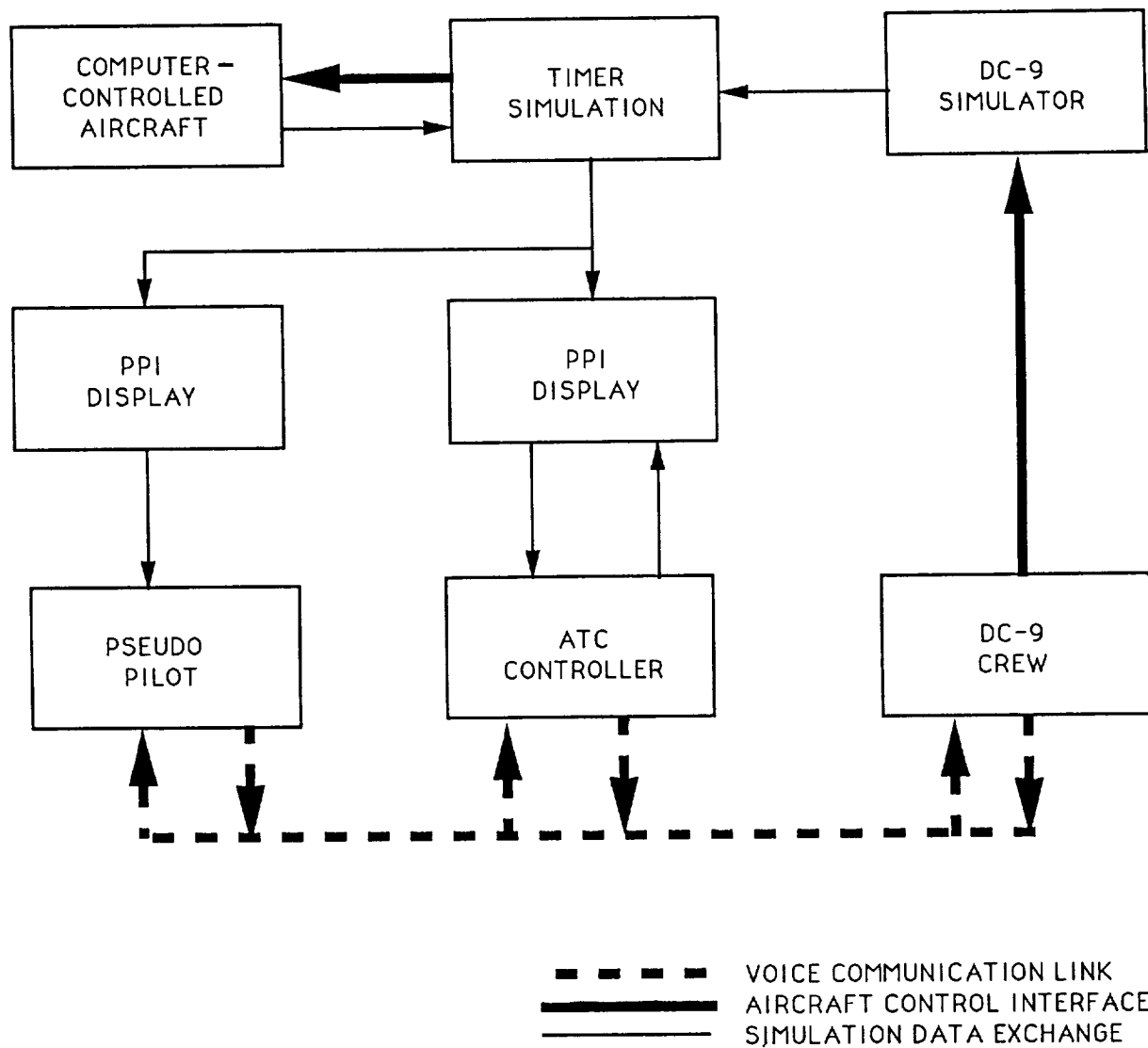
Figure 7. Interface diagram for experimental voice communication, aircraft control, and data exchange.
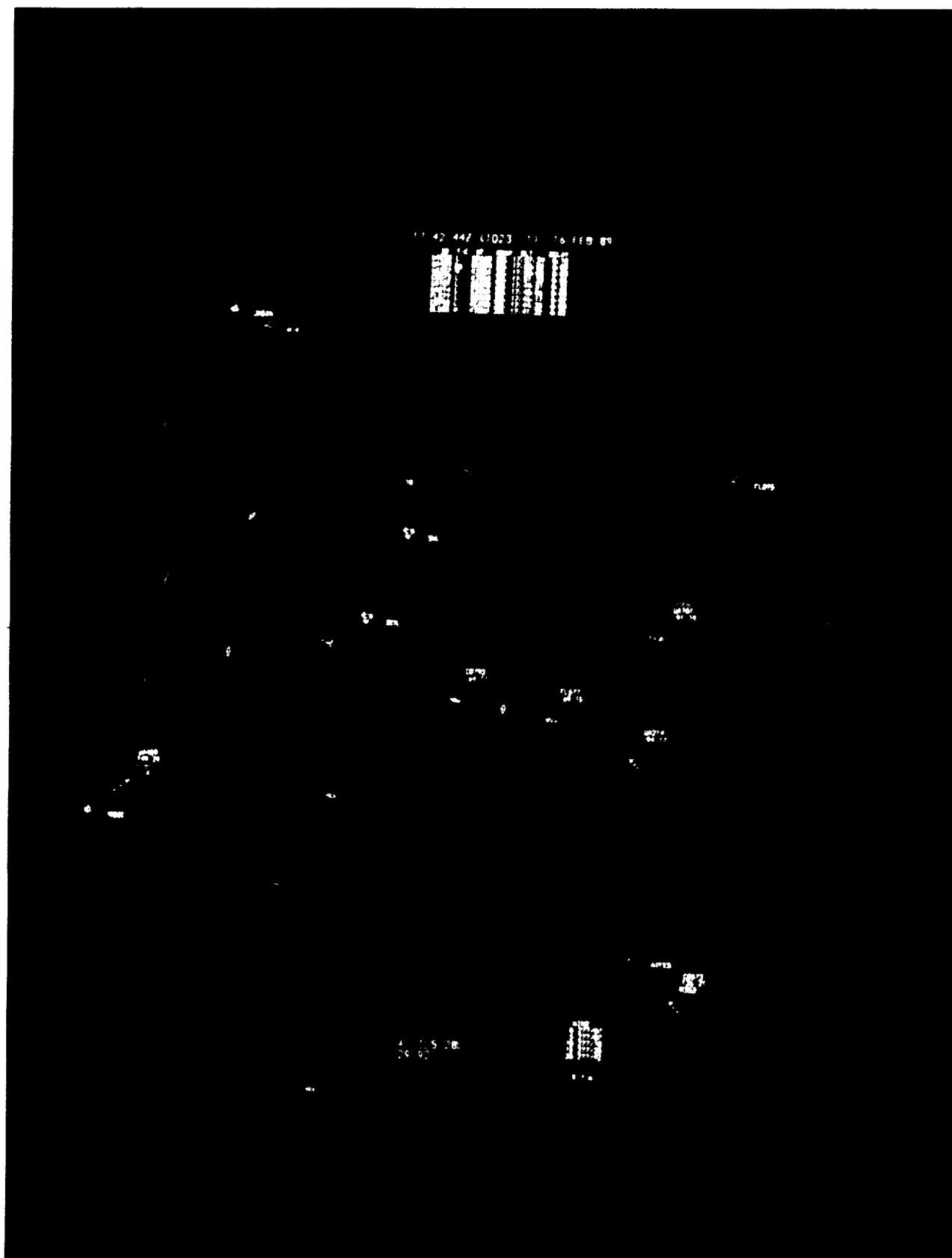
L-89-2566

Figure 8. Video map and aircraft positions on controller's display.

DRAKO ARRIVAL – RUNWAY 28L

DENVER ARR CON - 120.2
DENVER APP CON - 125.3
DENVER TOWER - - - 118.3
ATIS - - - - - - - - - - - - 125.6
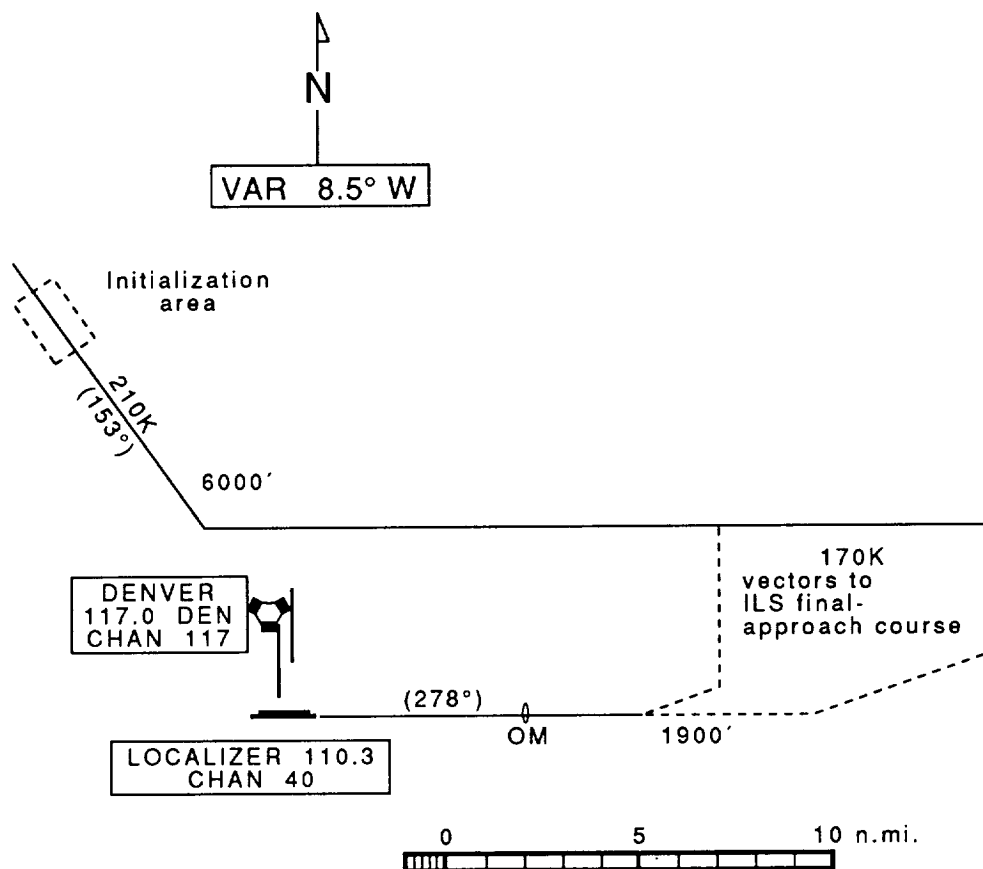
Figure 9. Nominal frequencies, speeds, headings, and altitudes for DRAKO arrival route of the Denver/Wallops terminal simulation area used in real-time simulation runs.

KEANN ARRIVAL — RUNWAY 28L

DENVER ARR CON - 120.2
DENVER APP CON - 125.3
DENVER TOWER --- 118.3
ATIS ------------ 125.6

Figure 10. Nominal frequencies, speeds, headings, and altitudes for KEANN arrival route of the Denver/Wallops terminal simulation area used in real-time simulation runs.
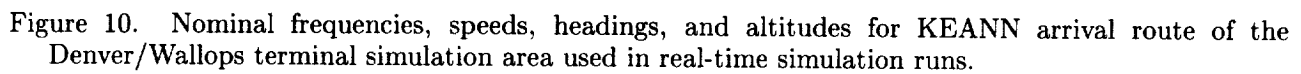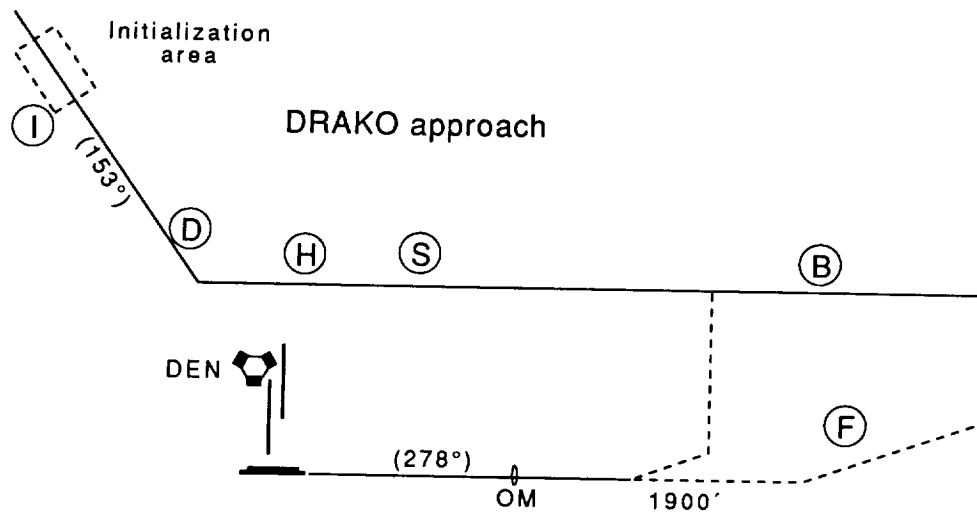
(a) DRAKO approach route.
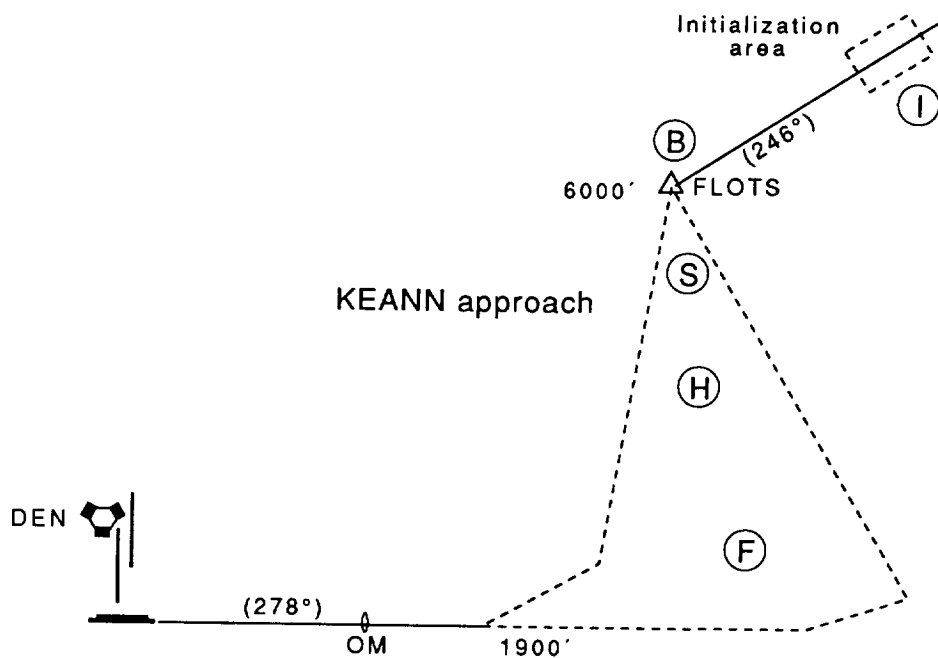
(b) KEANN approach route.

Figure 11. Event locations for two arrival routes flown in cockpit simulator.

Leader line

Aircraft symbol

Aircraft past-position markers

Note: Shaded areas indicate components of a normal ARTS III data block
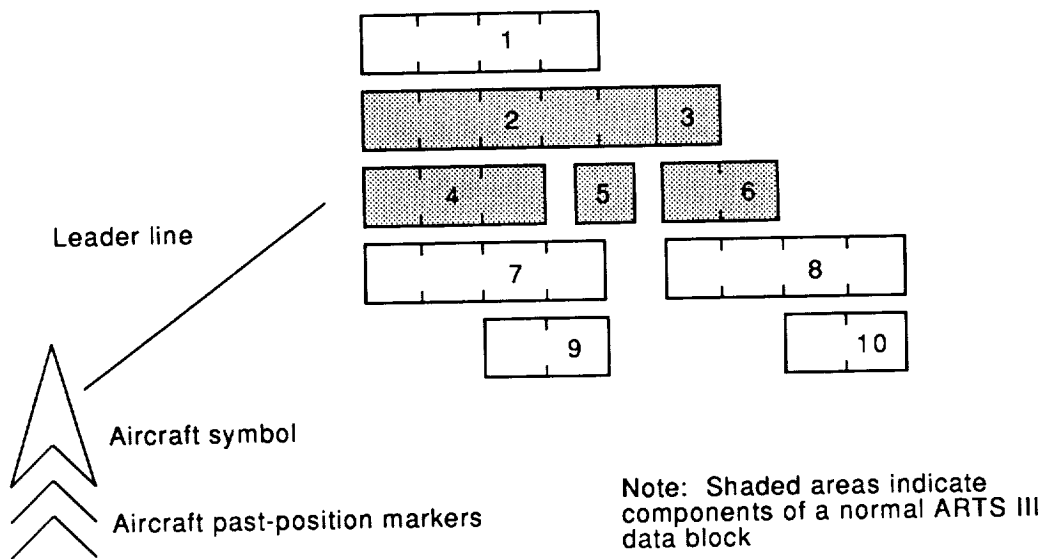
Data-tag fields

Field 1   DICE value   (e.g., +75   75 sec early at way point
                                                          -5   5 sec late at way point)

Field 2   Aircraft flight identification

Field 3   Symbol (H) for heavy jet

Field 4   Altitude / 100

Field 5   Handoff symbol

Field 6   Ground speed / 10

Field 7   Vector command   (e.g., L350   Left turn to 350°)

Field 8   Speed comand   (e.g., S190   Speed 190 knots)

Field 9   Countdown/countup time for field 7

Field 10   Countdown/countup time for field 8

Figure 12. Aircraft data-tag information for TIMER display.

28

UA422

110 23

Normal ARTS III Data Block: Top line - Aircraft call sign (United 422); Bottom line - altitude in feet / 100 (11000 ft), and ground speed in knots / 10 (230 knots).

UA422

110 23

L190

Command added on line below normal data block - 24 sec prior to transmittal time, the command (in this case a left turn to 190°) appears.

UA422

110 23

L190

Command begins flashing 12 sec prior to transmittal time.

UA422

110 23

L190

8

Countdown time appears on line below command, 8 sec prior to transmittal time; the command continues to flash.

UA422

110 23

L190

0

Countdown reaches zero; the command stops flashing; the command should be transmitted now; when transmission is made, a computer entry by the controller is required to remove the command and time from the data block.

UA422

110 23

L190

-1

Assuming that the computer entry is not made, the command continues to be displayed and the elapsed time since the transmission should have been made is indicated; additionally, the time will flash.

UA422

110 23

After the computer entry has been made, indicating that the controller no longer wants the information to be displayed, a normal data block returns.

Figure 13. Example of a series of data-tag information illustrating a vector control command.

AA641
110 23

Normal ARTS III data block.

+039
AA641

DICE value appears on line above the normal data block.

110 23

+035

AA641

110 23

Dice value decrements according to a comparison of the scheduled landing time to estimated aircraft arrival time. (Arrival time is a function of aircraft performance, tracker-estimated aircraft position, and estimated winds.)

●

●

(DICE value continues decrementing, +30, +025, +020 . . .)

●

+000
AA641
110 23
L350

DICE value goes to zero; the appropriate command appears in the line below the normal data block.

AA641
110 23
L350
-1

Elapsed time since the command should have been delivered appears in the line below the command; this count continues until the controller makes the appropriate computer entry.

AA641
110 23

After the computer entry has been made, indicating that the controller no longer wishes that the information be displayed, a normal data block returns.

Figure 14. Example of a series of data-tag information illustrating a DICE value countdown.

1. SET FD MODE/SEL OFF

2. SET AUTOTHROTTLE ON FOR TRIMMING

3. SET GEAR UP

4. SET FLAPS = 0°, SLATS = EXT

5. SET COMM HEAD #1 TO 120.2

6. SET NAV HEAD #1 TO 117.0

7. SET HSI COURSE
   (A) TO 246° (ROUTE #1)
   (B) TO 153° (ROUTE #4)

8. TELL COMPUTER OPERATOR - READY FOR INITIAL CONDITIONS

9. AFTER TRIM OCCURS AND RUN STARTS, DISENGAGE AUTOTHROTTLE AND FLY MANUAL THROTTLES

10. IF DESIRED SET FD MODE/SEL TO NAV/LOC

11. AT APPROPRIATE TIME DURING FLIGHT, TUNE ILS, NAV HEAD #1 TO 110.3 AND SET FD MODE/SEL TO APPR AUTO

12. TUNE COMM HEAD #1 AS DIRECTED BY ATC

13. CONFIGURE FOR APPROACH AT APPROPRIATE TIMES, USE FLAPS = 40° CONFIGURATION FOR LANDING, FLIP-CHART LANDING SPEED = 130 KNOTS

Figure 15. Simplified cockpit simulator procedure for a run.

PROFILE DESCENT RUNWAYS 10-19-28-1

DENVER/WALLOPS INTL
DENVER, *VIRGINIA*

EXPECT VECTOR TO FINAL APPROACH
PRIOR TO REACHING DENVER VORTAC

| FIX | FLYING MILES TO RUNWAY | | | |
	RWY 28	RWY 19	RWY 1	RWY 10
BENAM	70	55	70	55
SMITY	60	65	80	75
RAMAH	60	75	60	75
SHREW	70	75	55	55

J170

ESTUS

J56

53

BENAM

58

R.333

Cross at or between *FL 180*
and *12,000'* at *250 K.* Descend
and maintain *8,000'*.

DRAKO

153°
(33)

R.353

Cross at or between *FL 180*
and *12,000'* at *250 K.* Descend
and maintain *7,000'*.

J157

J110 J114 J172

R.066

58

SMITY

I-HMX LOC 111.1

DENVER
117.0 DEN 117

246°
(34)

R.016

KEANN

I-GQW LOC 111.5   R.233   R.128   I-DEN LOC 110.3

053°
(36)

318°
(34)

KIOWA
117.5 IOC 122

BYSON

KIOWA

R.233

I-SPO LOC 110.7   I-RRV LOC 109.3

SHREW

53

Cross at or between *FL 180*
and *12,000'* at *250 K.* Descend
and maintain *9,000'*.

R.145

27

RAMAH

110-130-44

J168-171

Cross at or between *FL 180*
and *12,000'* at *250 K.* Descend
and maintain *6,000'*.

NOTE: In the event of lost communications, FAR 91.127
applicable.

RADAR AND DME REQUIRED

NOTE: Chart not to scale.

PROFILE DESCENT RUNWAYS 10-19-28-1

DENVER, *VIRGINIA*
DENVER/WALLOPS INTL

Figure 16. Profile descent navigation chart of terminal area simulated.

Figure 17. ILS approach plate of terminal area simulated.
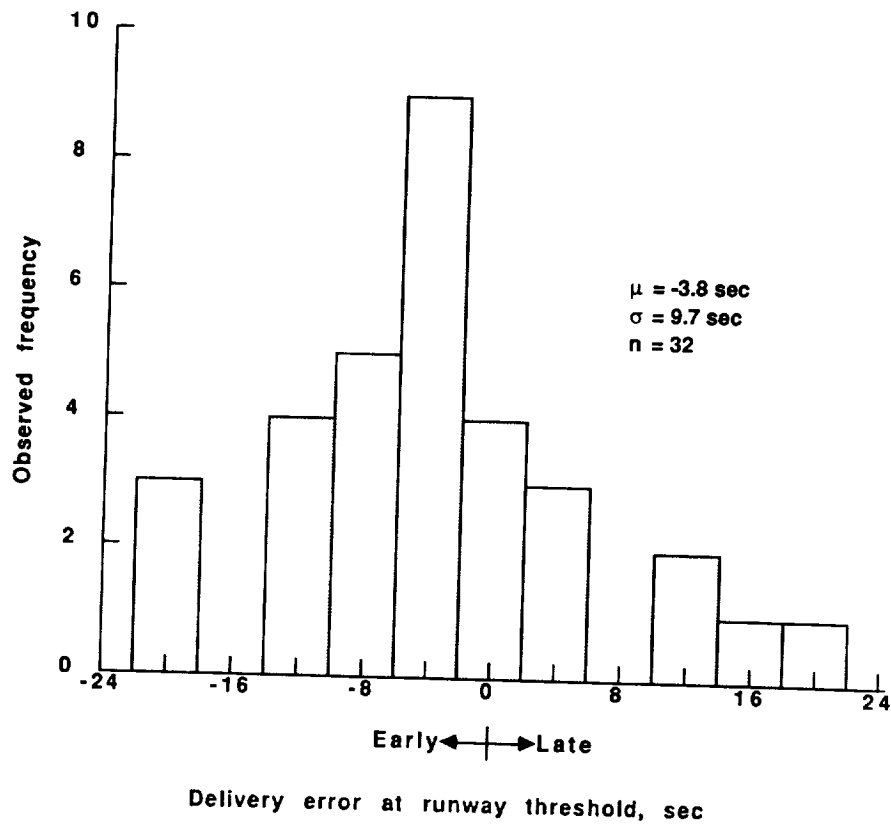
Figure 18. Frequency distribution of single-aircraft, runway-threshold delivery-time errors for runs before TIMER briefing to crew.
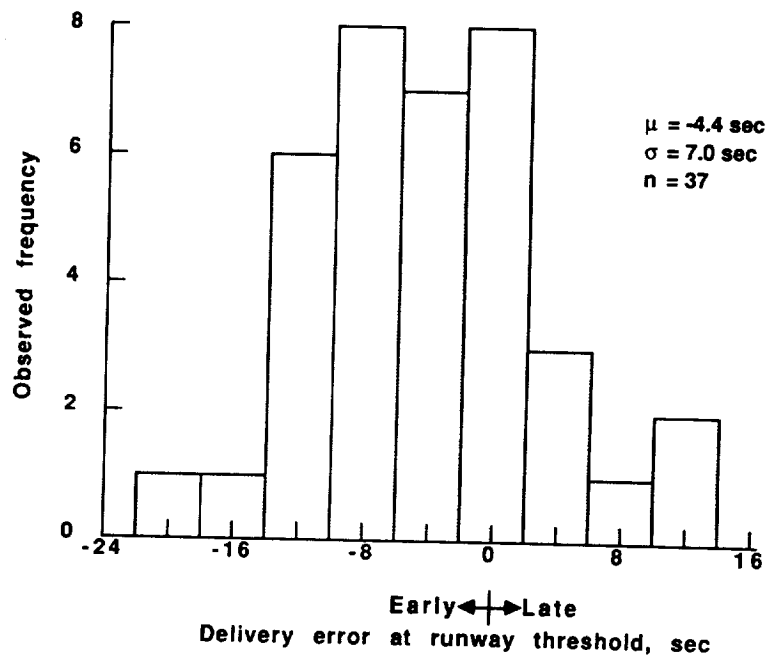
Figure 19. Frequency distribution of single-aircraft, runway-threshold delivery-time errors for runs after TIMER briefing to crew.
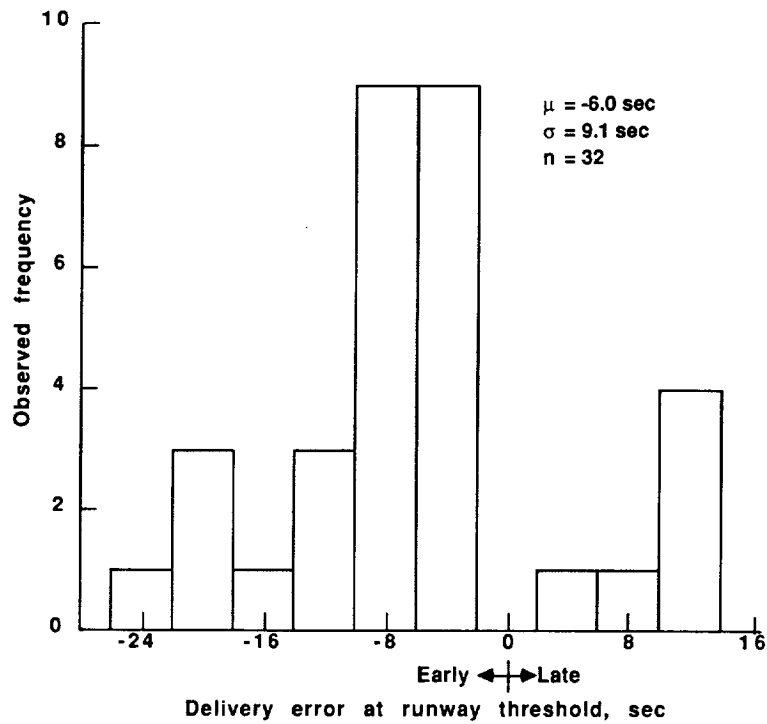
Figure 20. Frequency distribution of single-aircraft, final-approach-fix delivery-time errors for runs before TIMER briefing to crew.
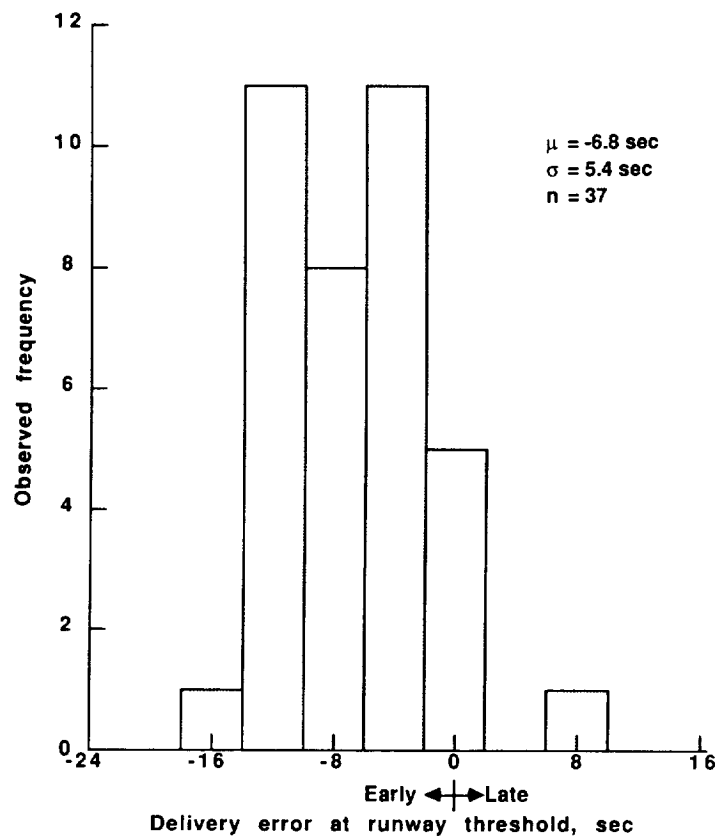
Figure 21. Frequency distribution of single-aircraft, final-approach-fix delivery-time errors for runs after TIMER briefing to crew.

35
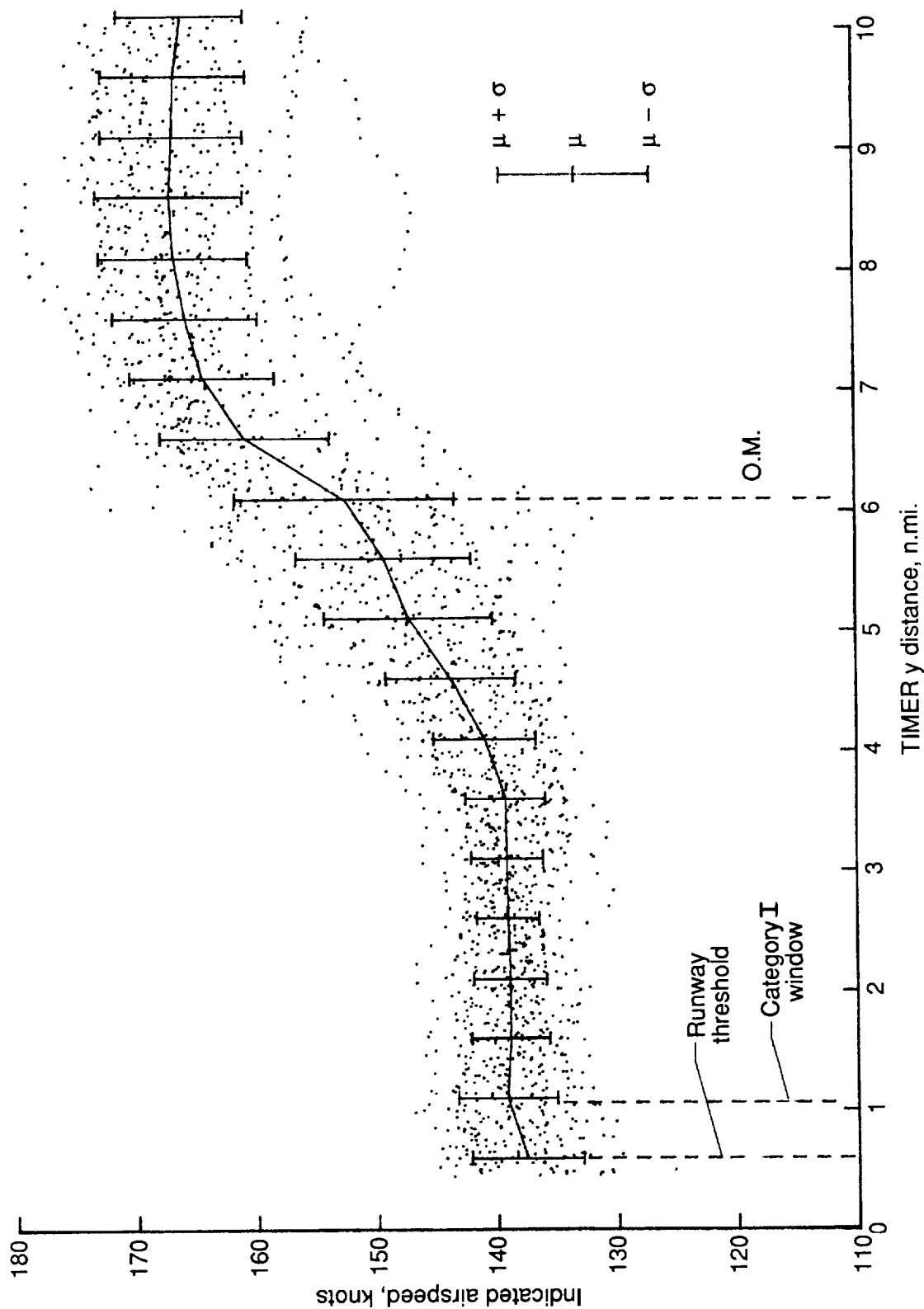
Figure 22. Distribution of indicated airspeeds for DC-9 simulator along final approach for runs before TIMER briefing to crew. The y distance is relative to TIMER north axis.
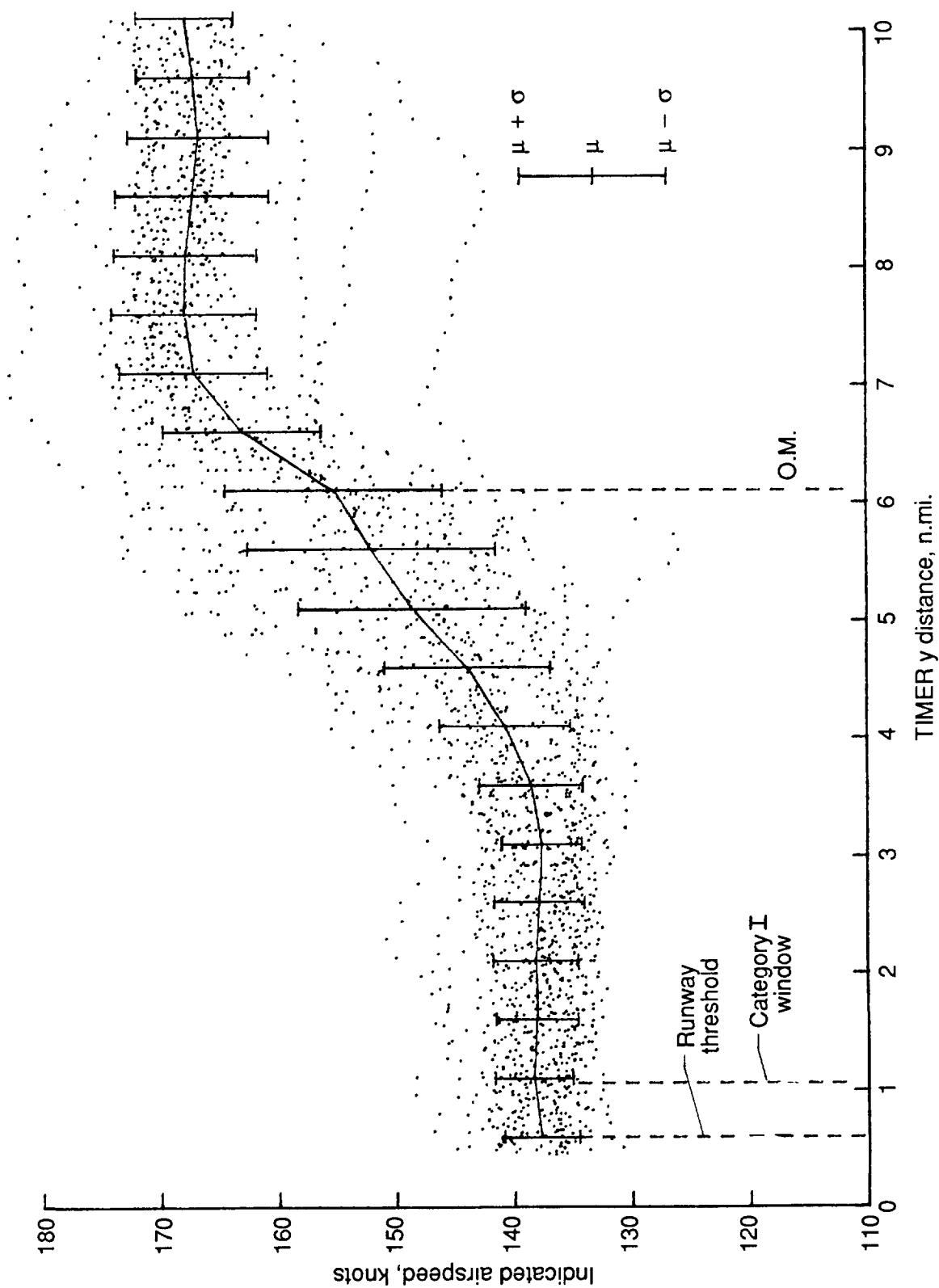
Figure 23. Distribution of indicated airspeeds for DC-9 simulator along final approach for runs after TIMER briefing to crew. The *y* distance is relative to TIMER north axis.

μ = 139.2 knots
σ = 4.1 knots
n = 31

Indicated airspeed at Category I window, knots
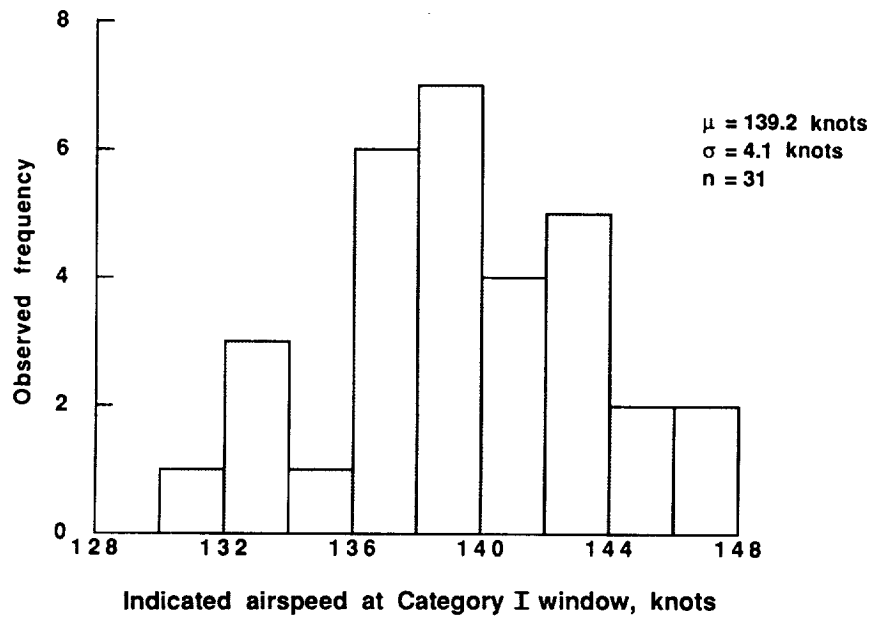
Figure 24. Frequency distribution of indicated airspeed at ILS Category I window for runs before TIMER briefing to crew.

μ = 138.4 knots
σ = 3.3 knots
n = 37

Indicated airspeed at Category I window, knots
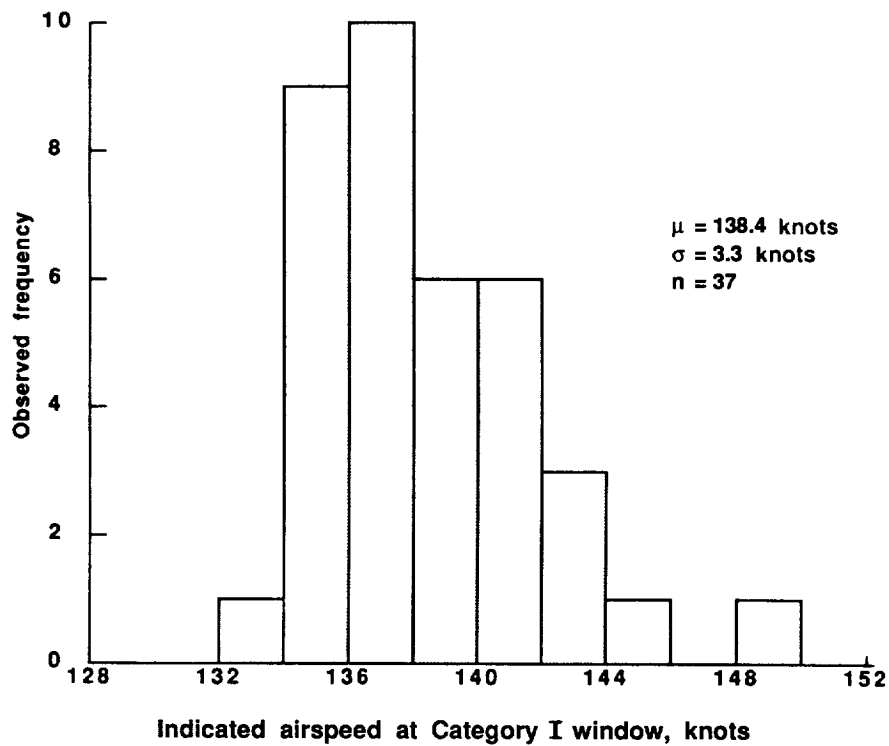
Figure 25. Frequency distribution of indicated airspeed at ILS Category I window for runs after TIMER briefing to crew.

38
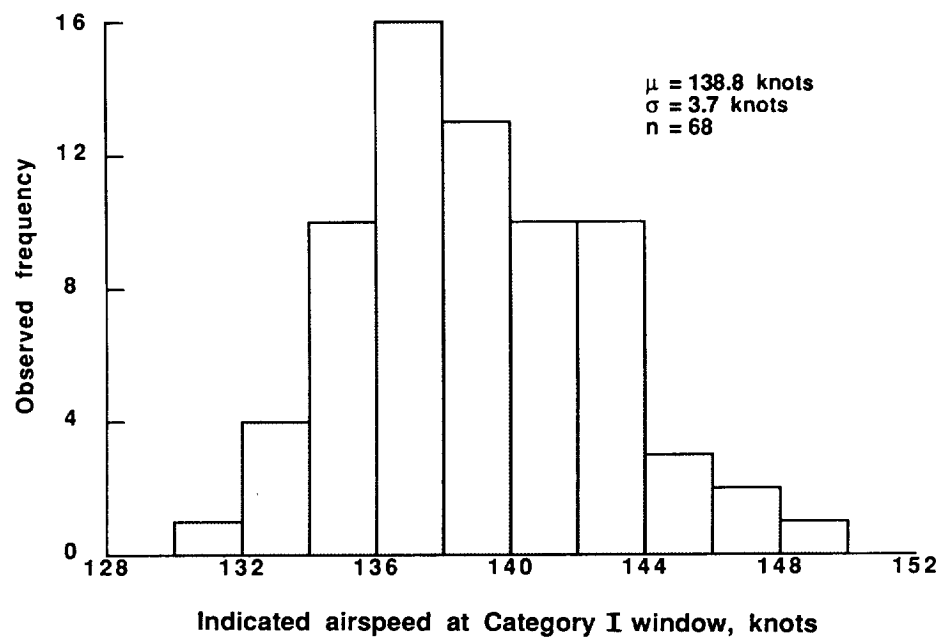
Figure 26. Frequency distribution of indicated airspeed at ILS Category I window for combined (before and after) TIMER briefing runs.
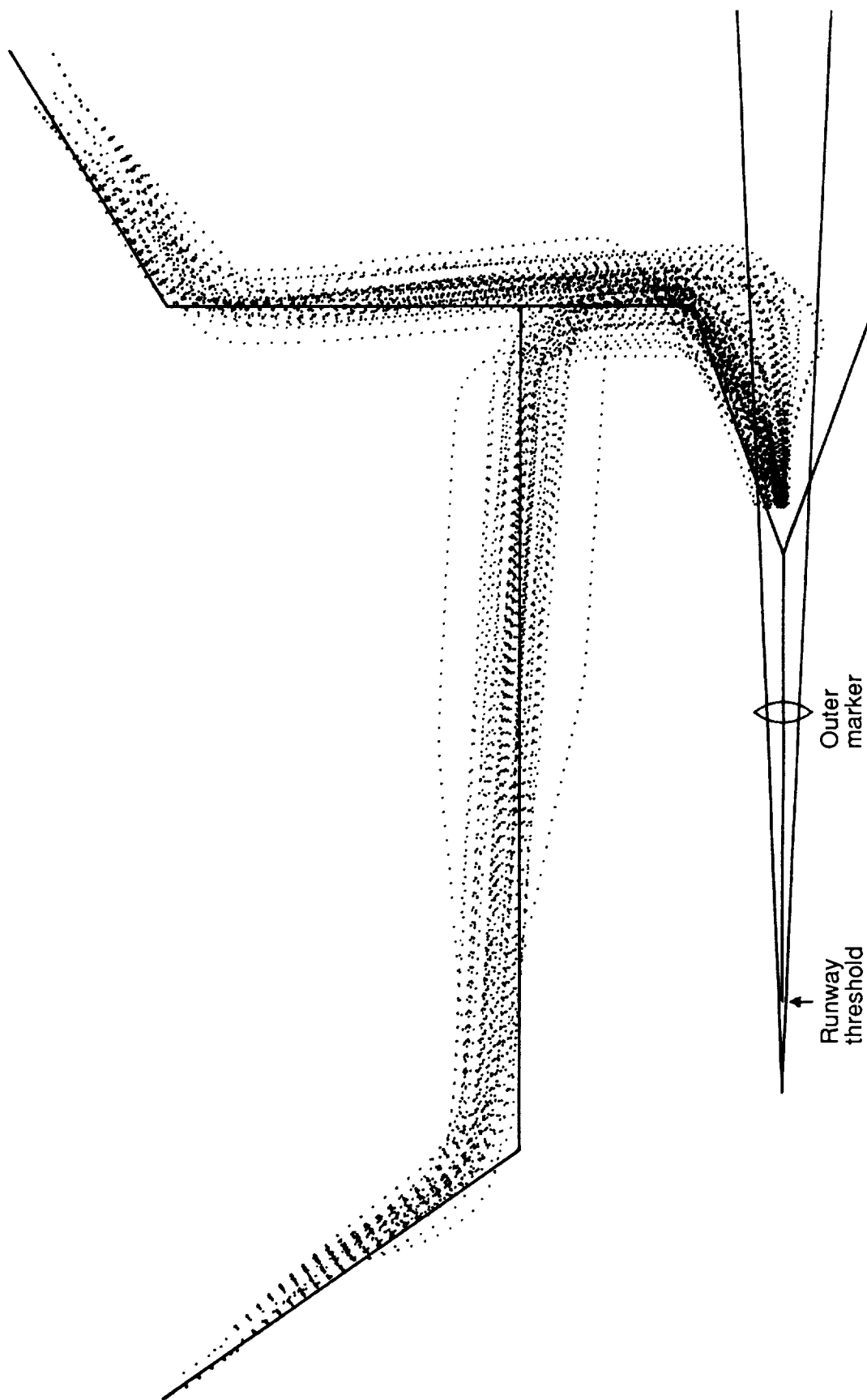
Figure 27. Superimposition of arrival paths flown to final-approach area for all data runs.
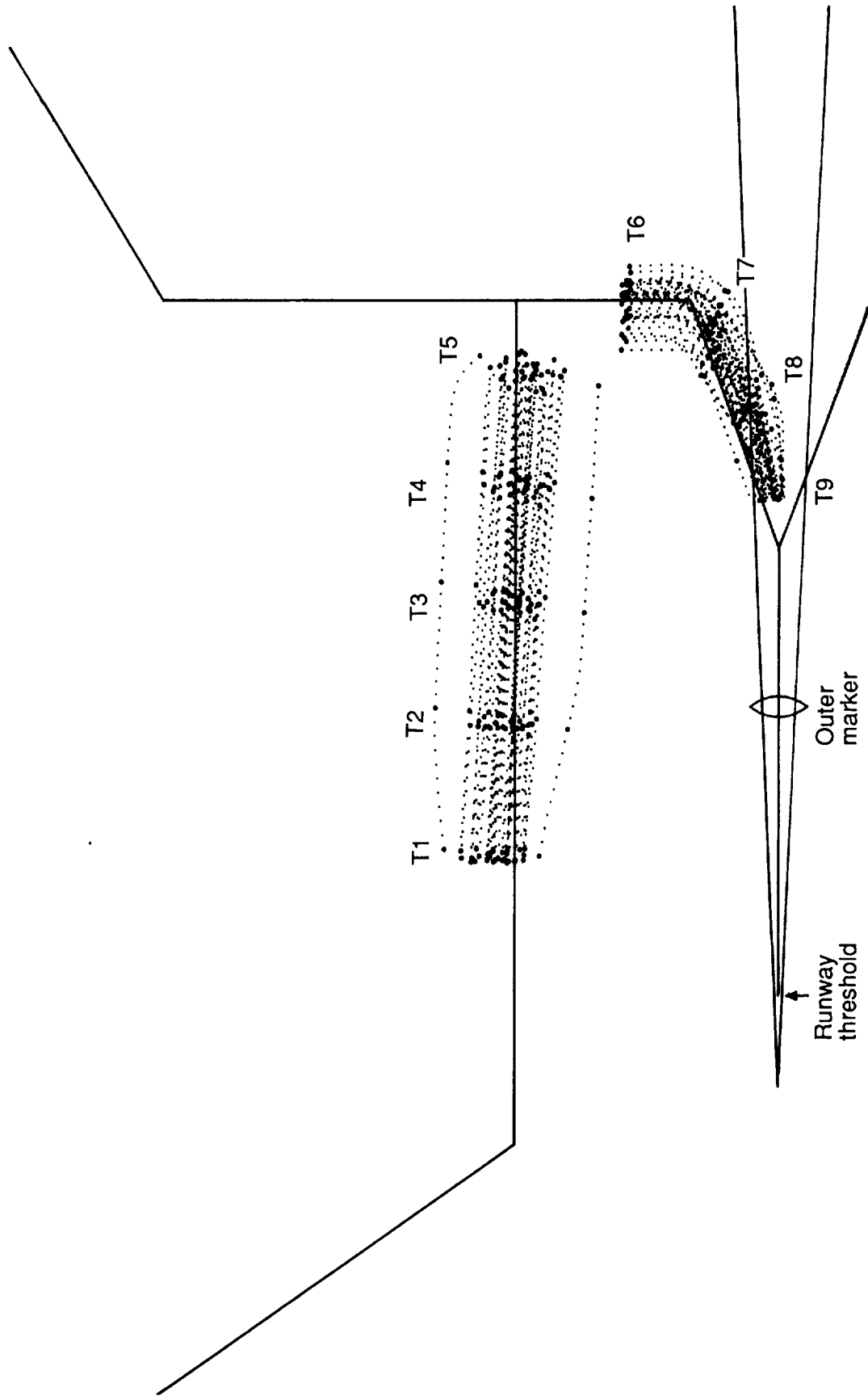
Figure 28. Superimposition of two segments of paths flown for all KEANN data runs with periodic aircraft locations, at reference time points, indicated for speed correlation in figure 29.
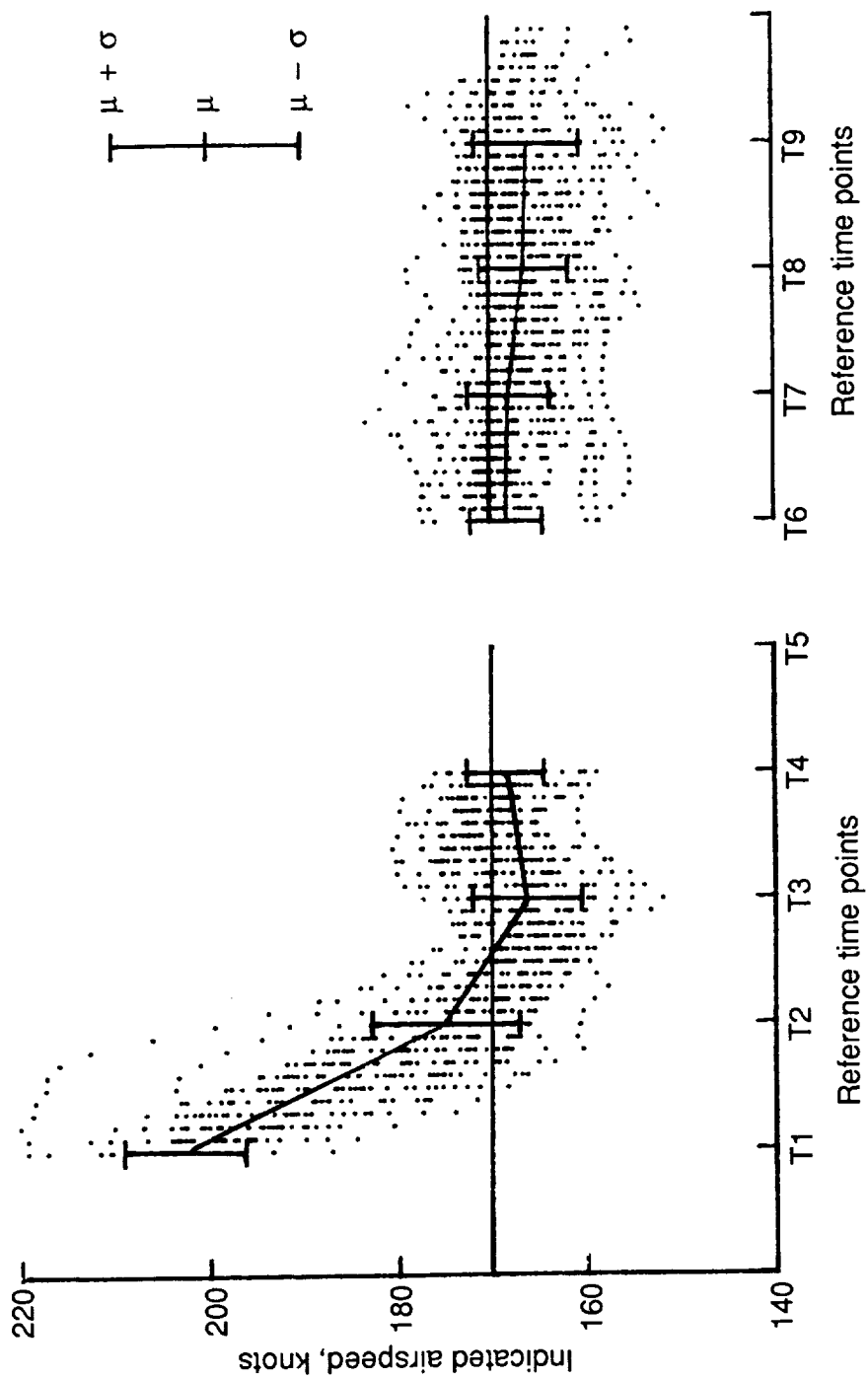
Figure 29. Indicated airspeeds along two segments of KEANN approach corresponding to path positions shown in figure 28.
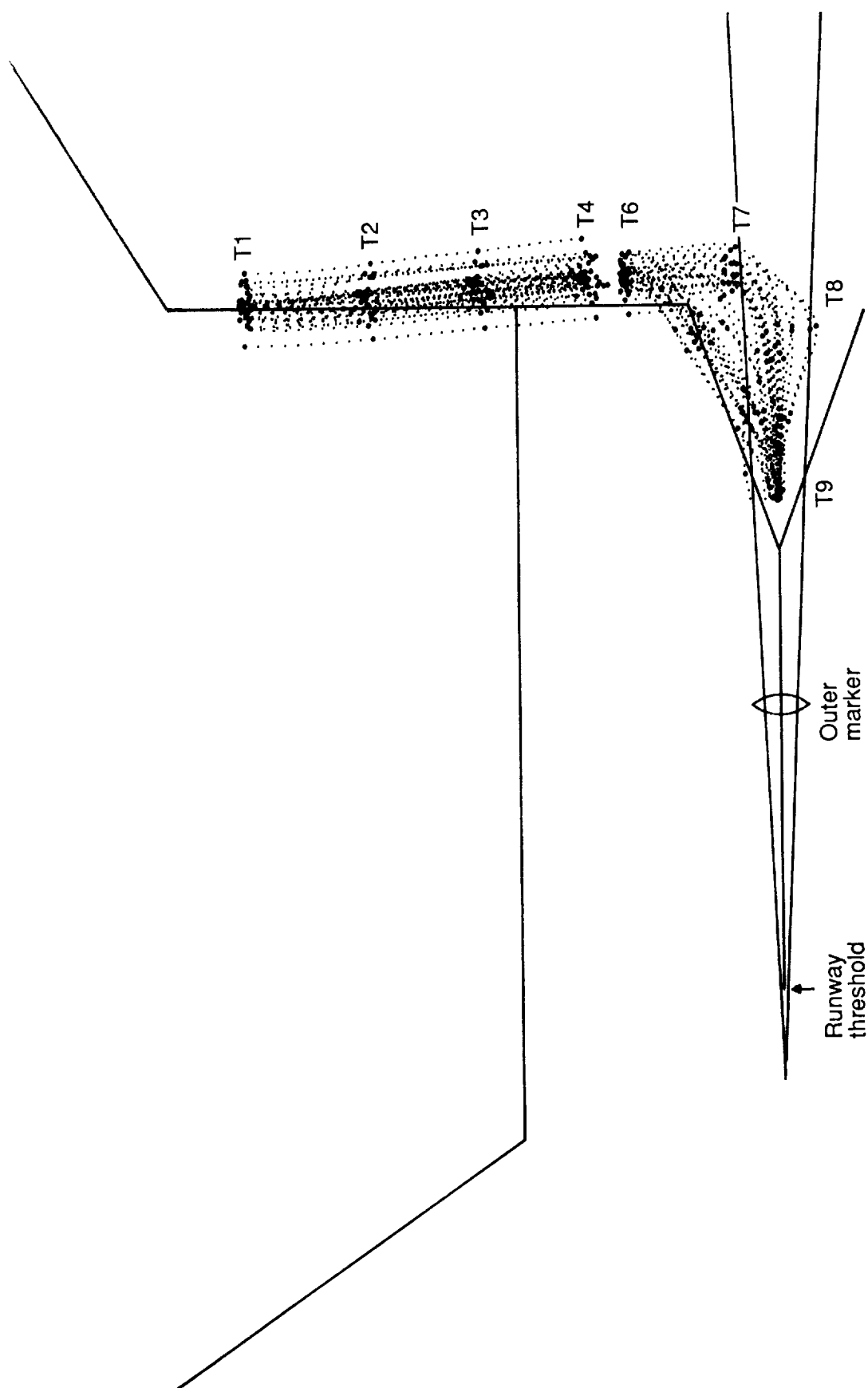
Figure 30. Superimposition of two segments of paths flown for all DRAKO data runs with periodic aircraft locations, at reference time points, indicated for speed correlation in figure 31.
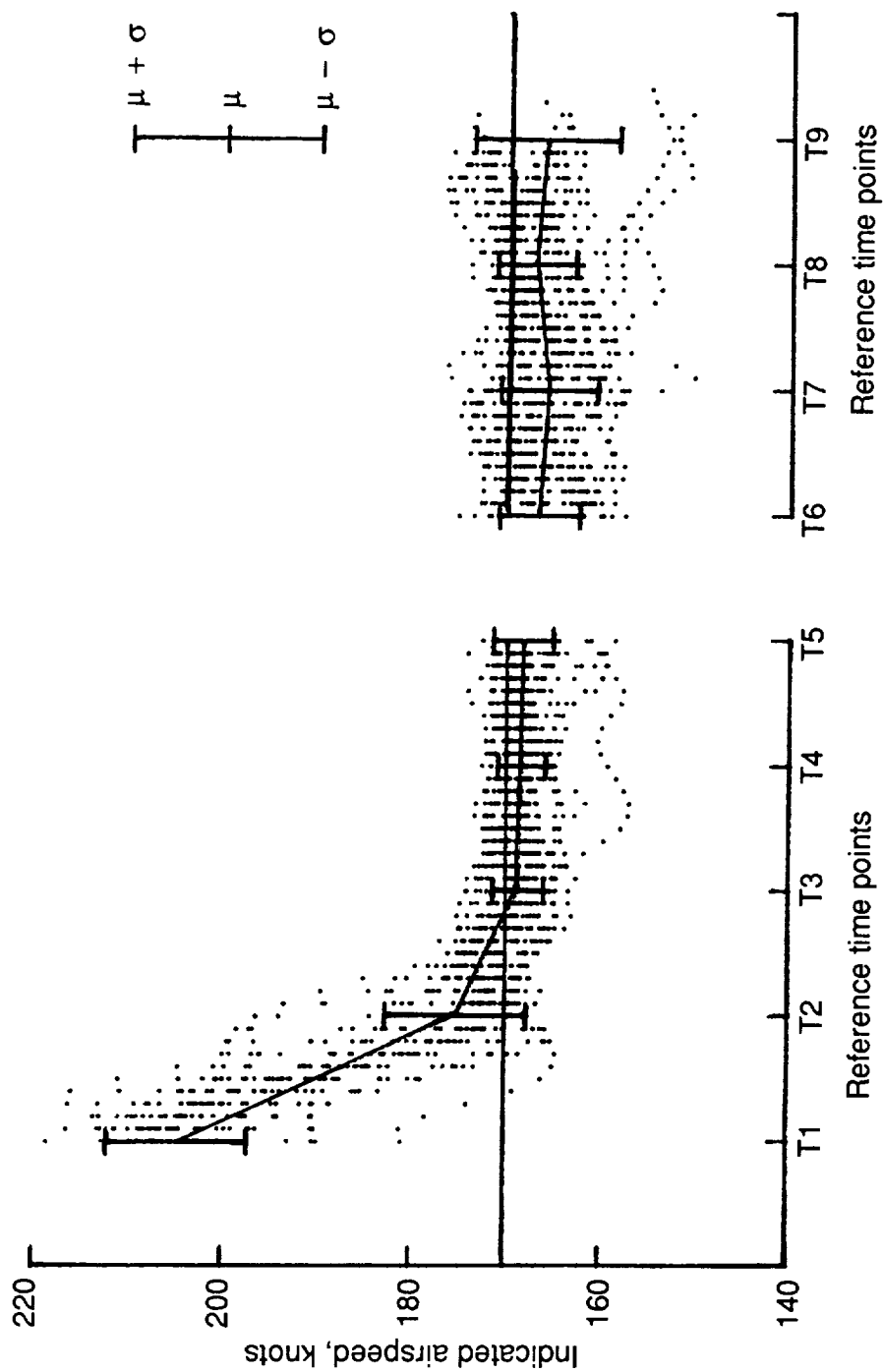
Figure 31. Indicated airspeed along two segments of DRAKO approach corresponding to path positions shown in figure 30.

μ = 3.1 sec
σ = 1.7 sec
n = 28
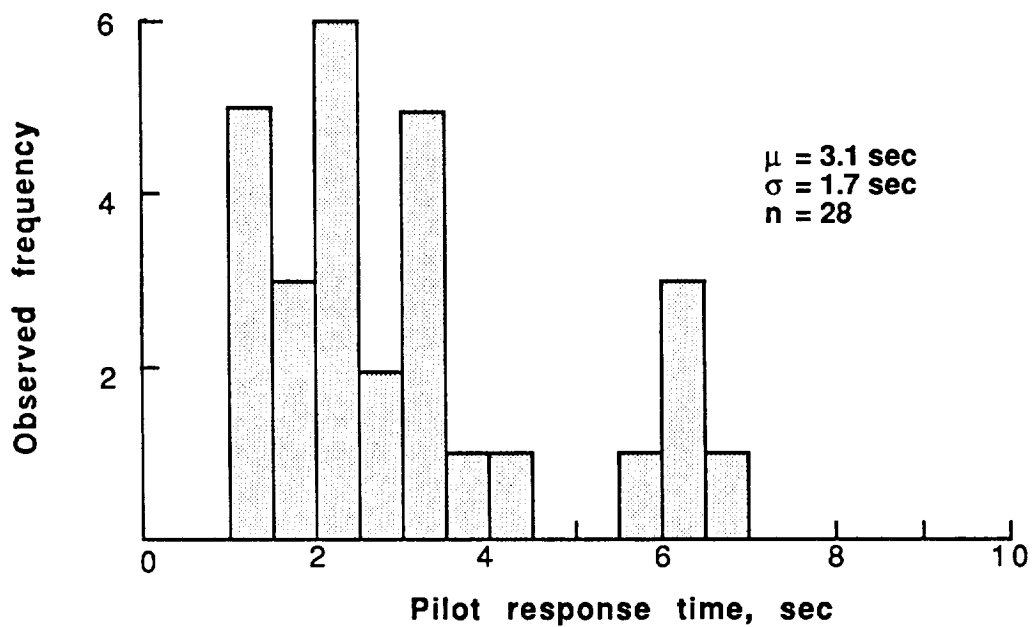
Figure 32. Frequency distribution of turn-to-final response time for runs before TIMER briefing to crew.

μ = 3.1 sec
σ = 2.2 sec
n = 34
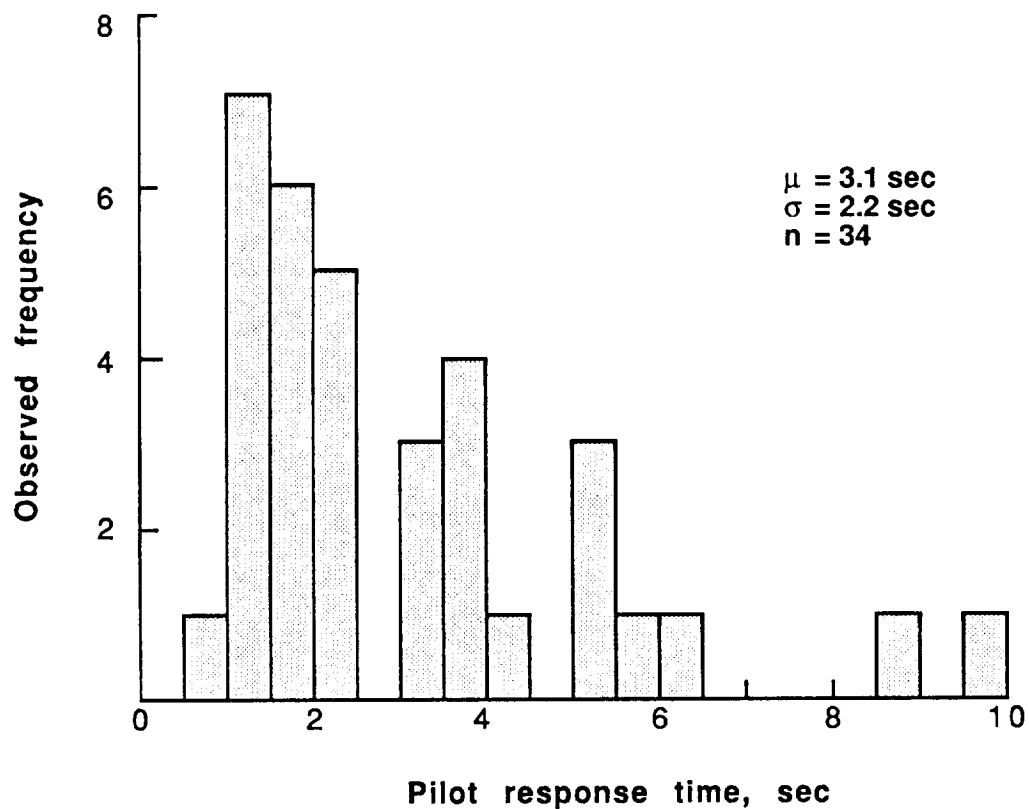
Figure 33. Frequency distribution of turn-to-final response time for runs after TIMER briefing to crew.

μ = 3.1 sec
σ = 2.0 sec
n = 62

$$f_x(t) = \frac{\beta}{\eta}\left(\frac{t-\gamma}{\eta}\right)^{\beta-1} \exp\left[-\left(\frac{t-\gamma}{\eta}\right)^{\beta}\right] \quad (t \geq \gamma)$$

$$f_x(t) = 0 \qquad (t < \gamma)$$

$\gamma = 0.9, \beta = 1.1, \eta = 2.28$

Probability

Pilot response time, sec
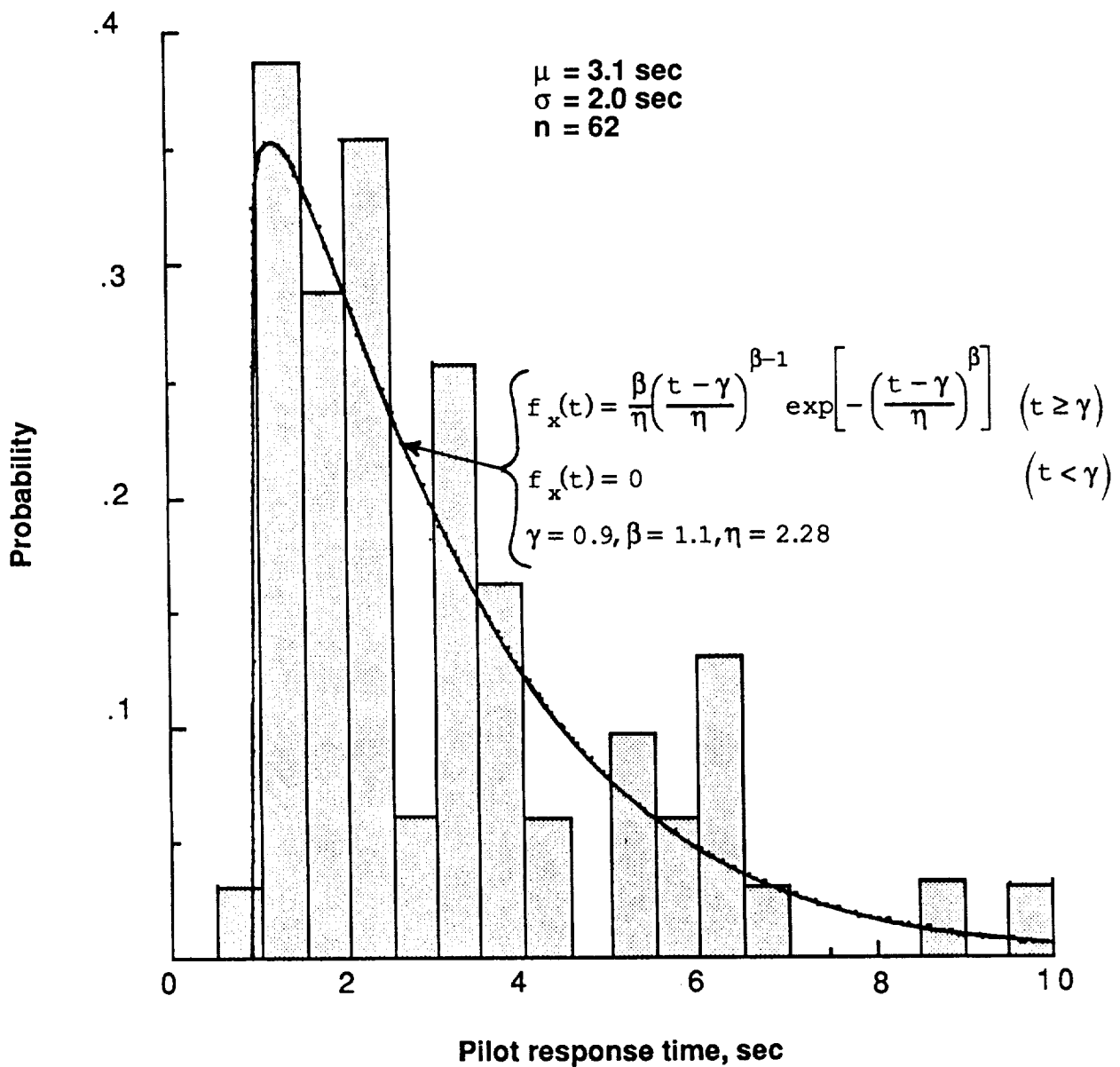
Figure 34. Histogram of turn-to-final response time for combined (before and after TIMER briefing) runs with fitted Weibull density.
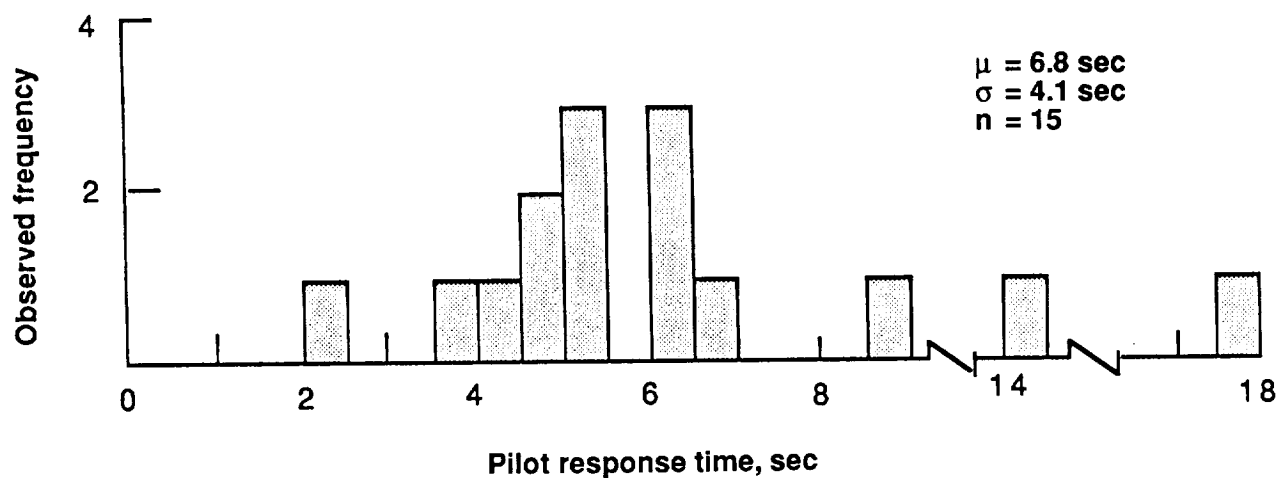
Figure 35. Frequency distribution of KEANN turn-to-base response time for runs before TIMER briefing to crew.
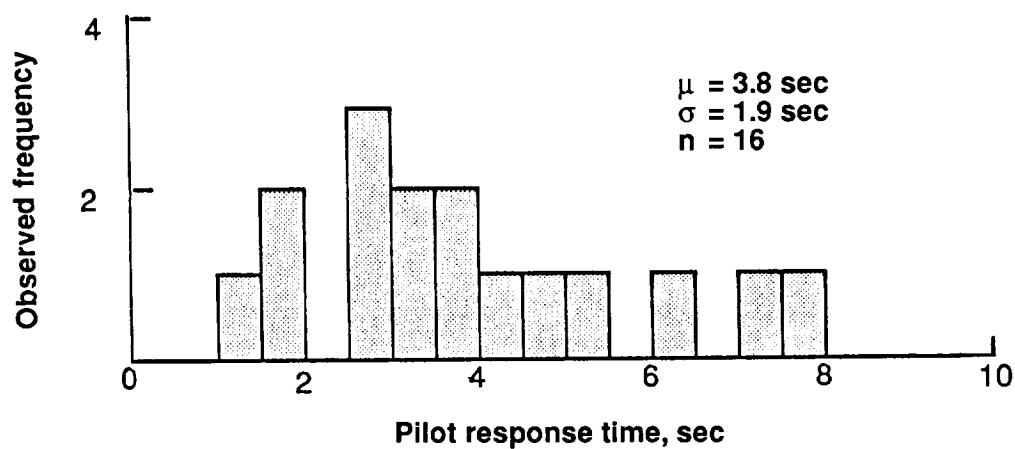
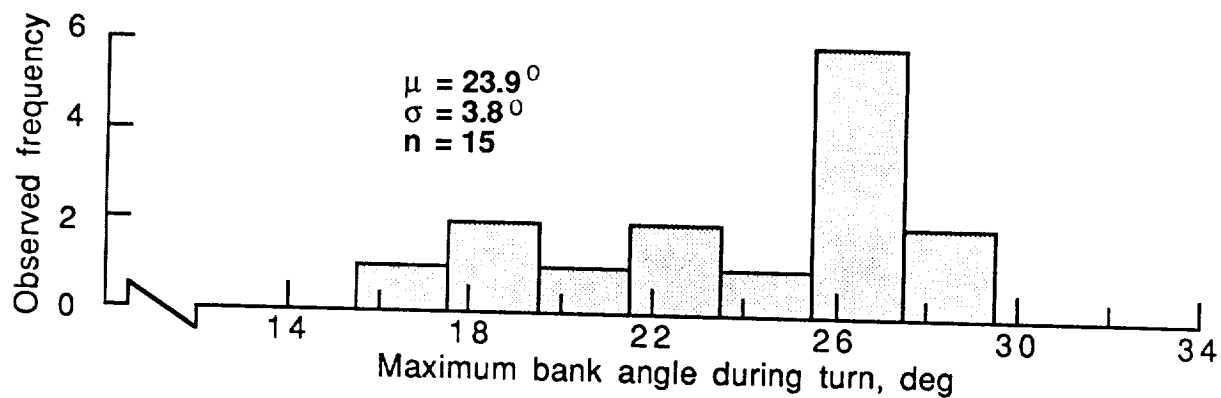Figure 36. Frequency distribution of KEANN turn-to-base response time for runs after TIMER briefing to crew.
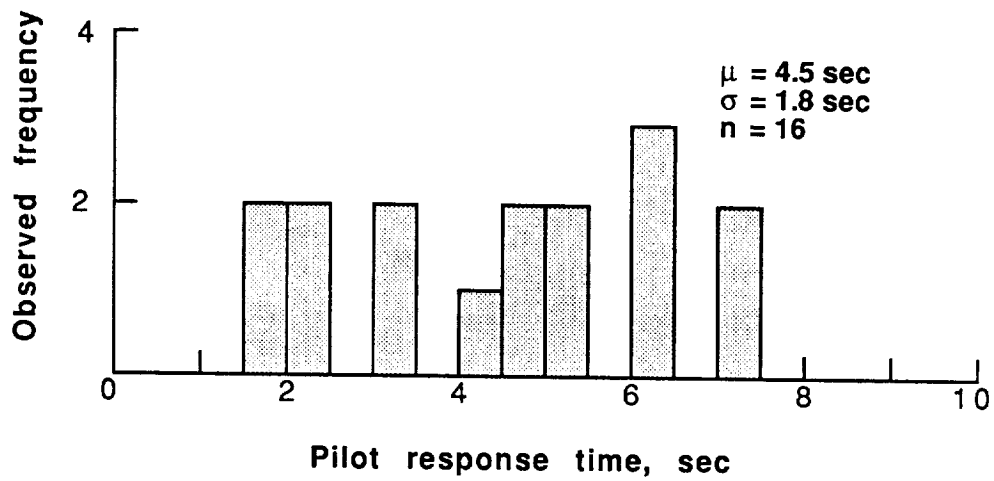
Figure 37. Frequency distribution of DRAKO turn-to-downwind response time for runs before TIMER briefing to crew.
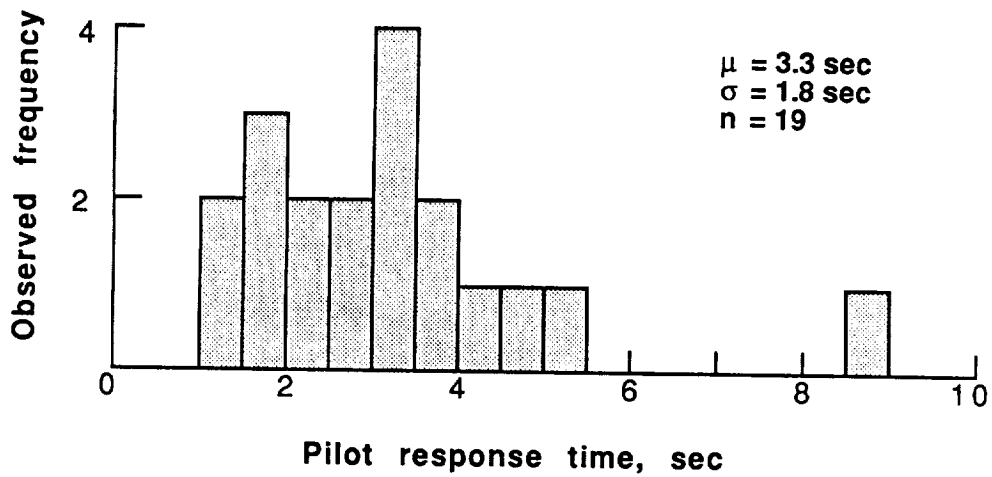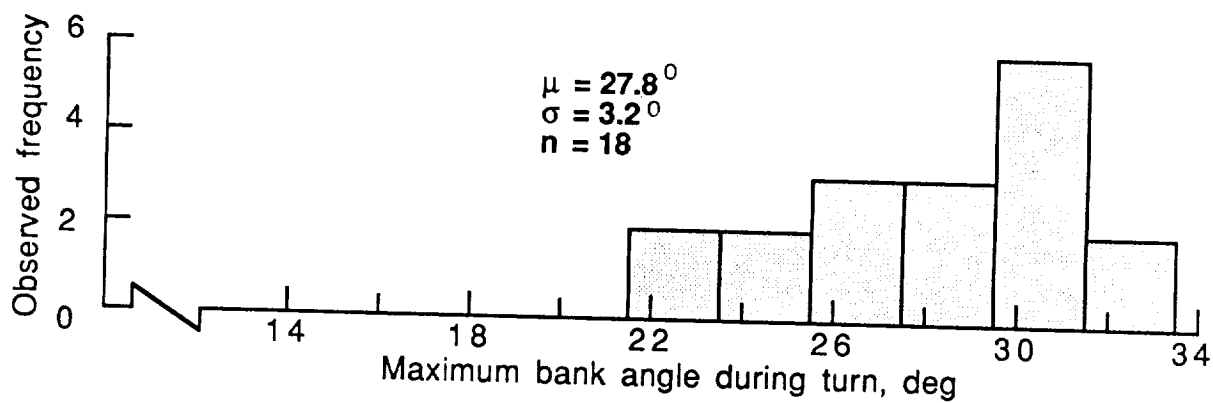

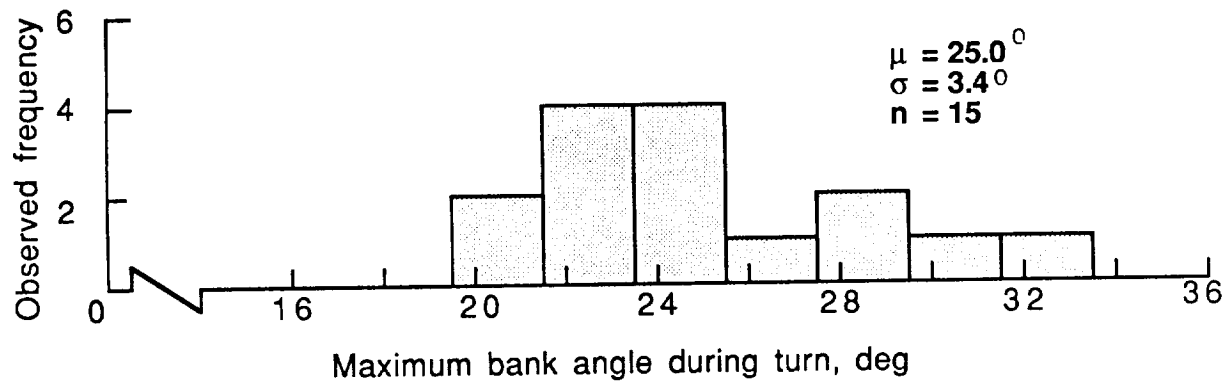Figure 38. Frequency distribution of DRAKO turn-to-downwind response time for runs after TIMER briefing to crew.

48
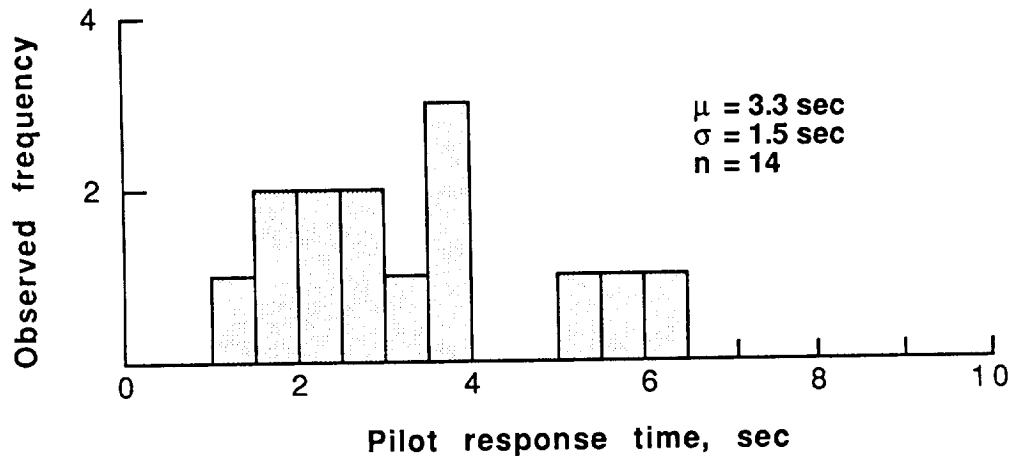
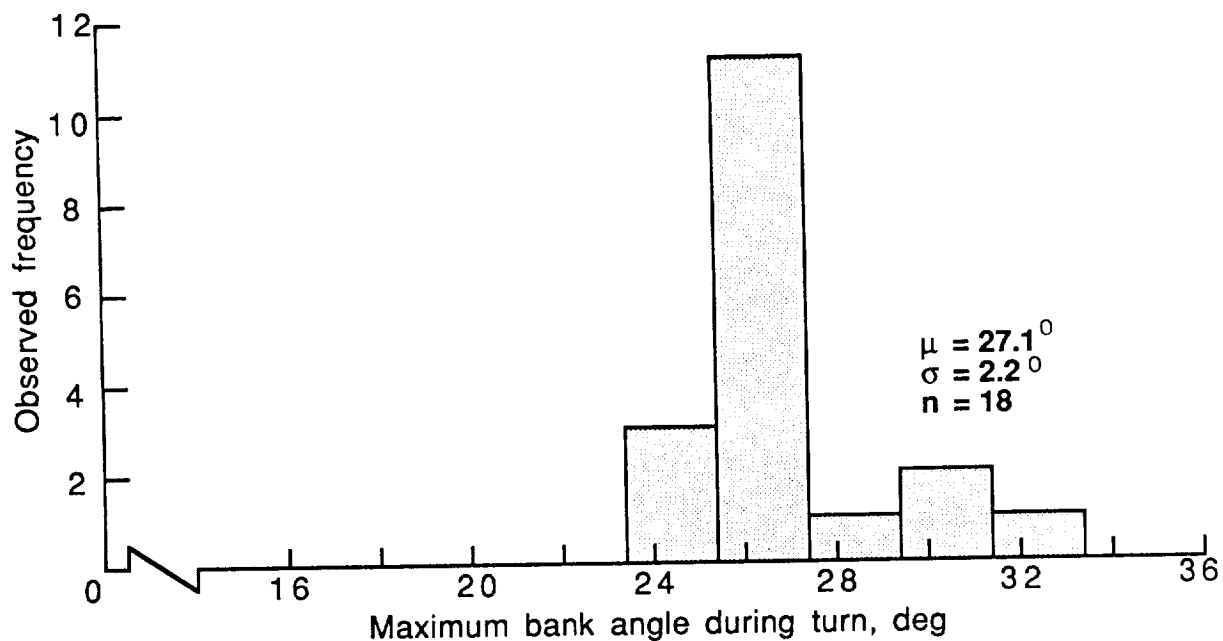Figure 39. Frequency distribution of DRAKO turn-to-base response time for runs before TIMER briefing to crew.
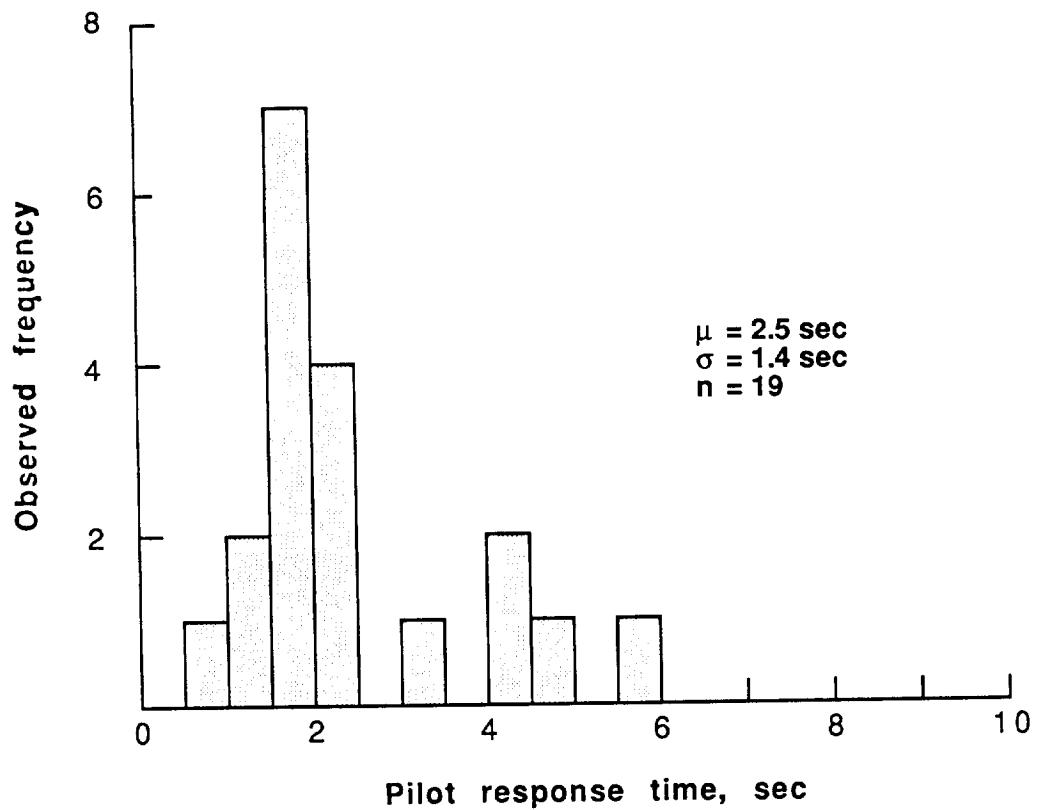
Figure 40. Frequency distribution of DRAKO turn-to-base response time for runs after TIMER briefing to crew.
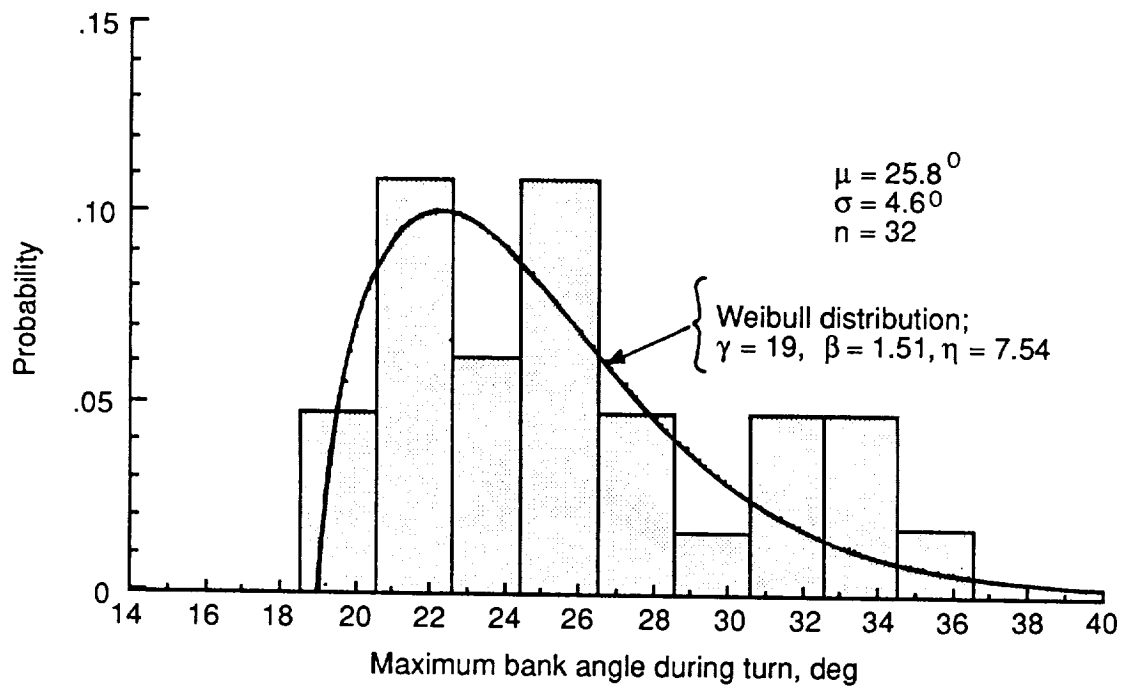
Figure 41. Histogram of turn-to-final bank angles for runs before TIMER briefing to crew with fitted Weibull density.
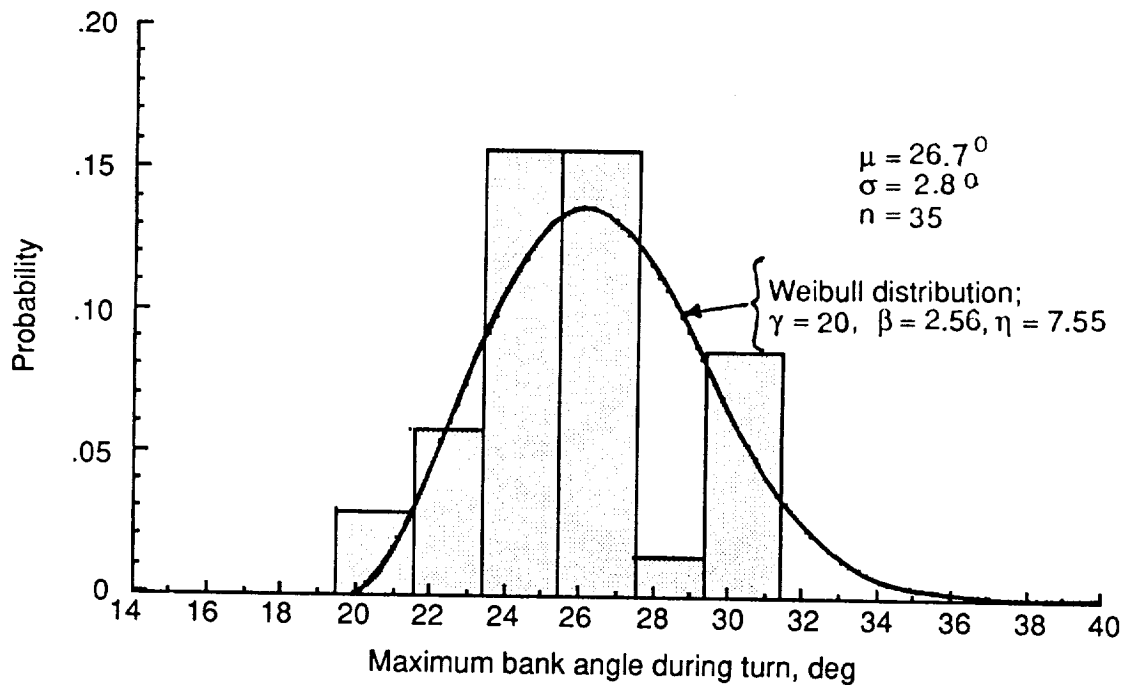
Figure 42. Histogram of turn-to-final bank angles for runs after TIMER briefing to crew with fitted Weibull density.
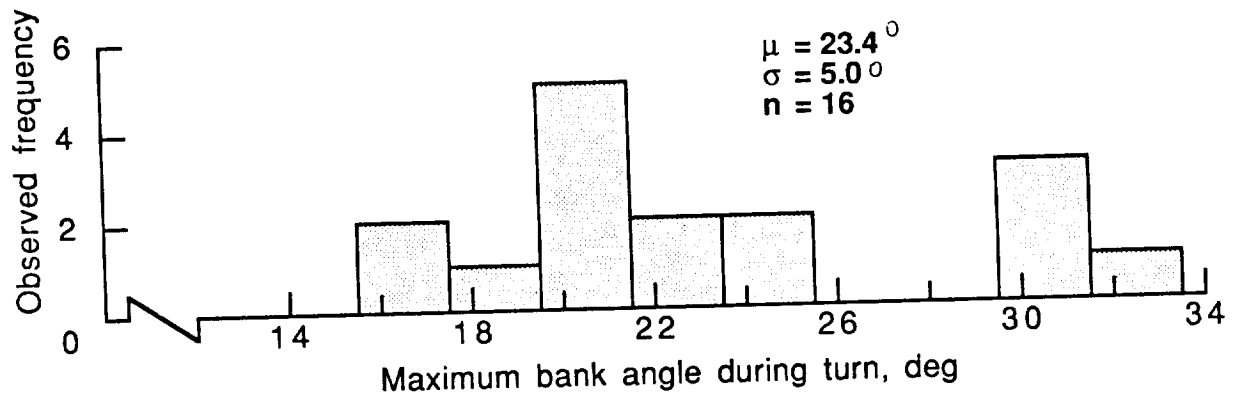
Figure 43. Frequency distribution of KEANN turn-to-base bank angle for runs before TIMER briefing to crew.
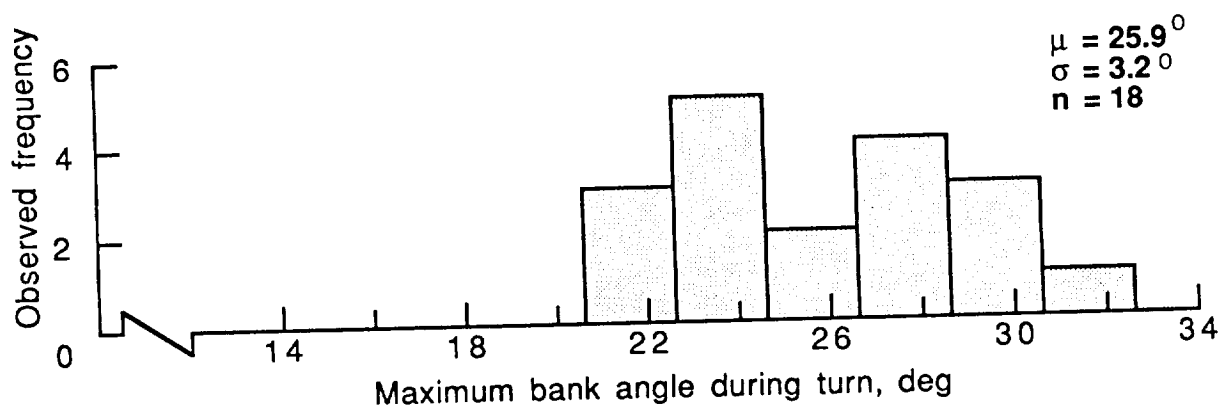
Figure 44. Frequency distribution of KEANN turn-to-base bank angle for runs after TIMER briefing to crew.

Figure 45. Frequency distribution of DRAKO turn-to-downwind bank angle for runs before TIMER briefing to crew.

Figure 46. Frequency distribution of DRAKO turn-to-downwind bank angle for runs after TIMER briefing to crew.

Figure 47. Frequency distribution of DRAKO turn-to-base bank angle for runs before TIMER briefing to crew.

Figure 48. Frequency distribution of DRAKO turn-to-base bank angle for runs after TIMER briefing to crew.
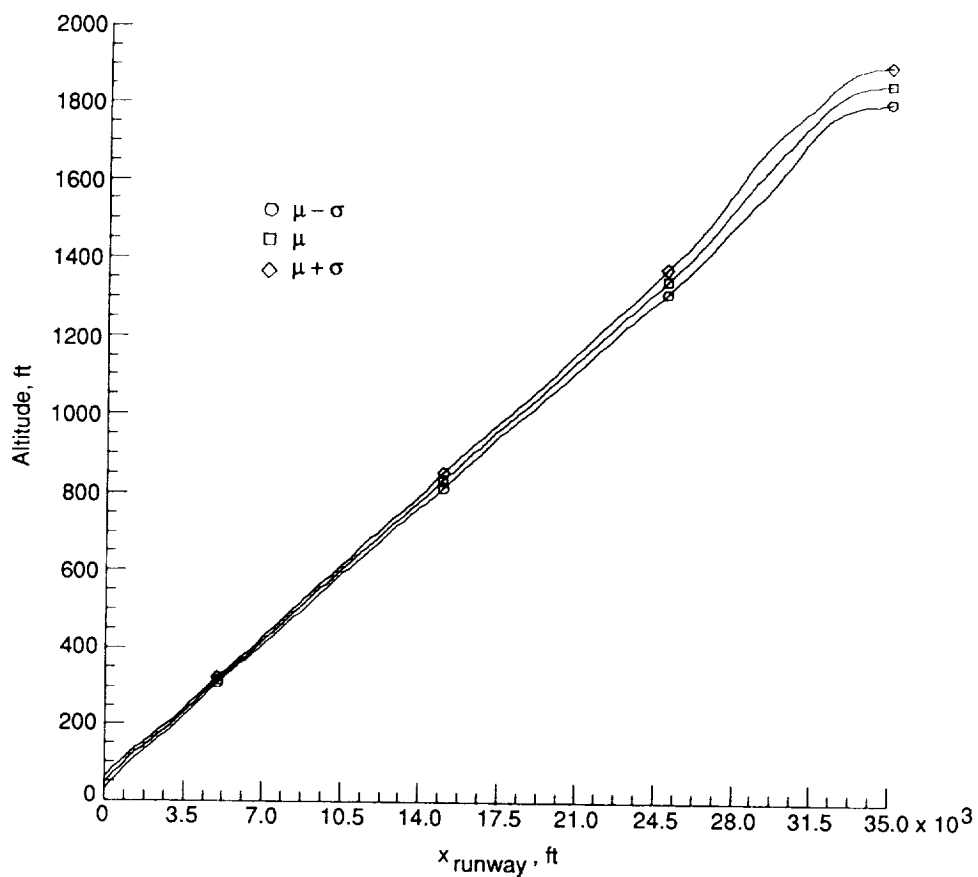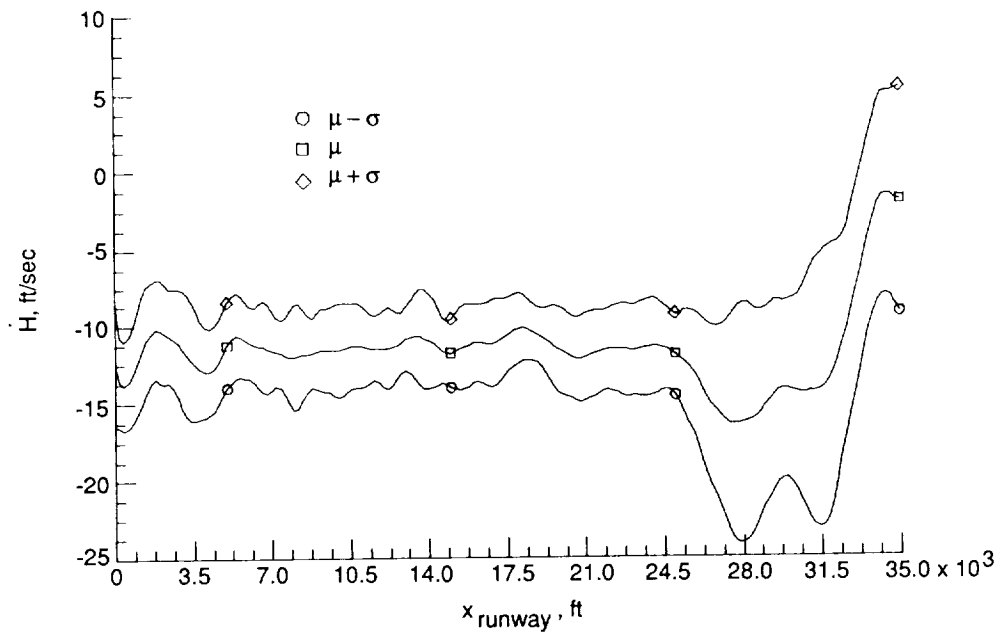
(a) Altitude profile.
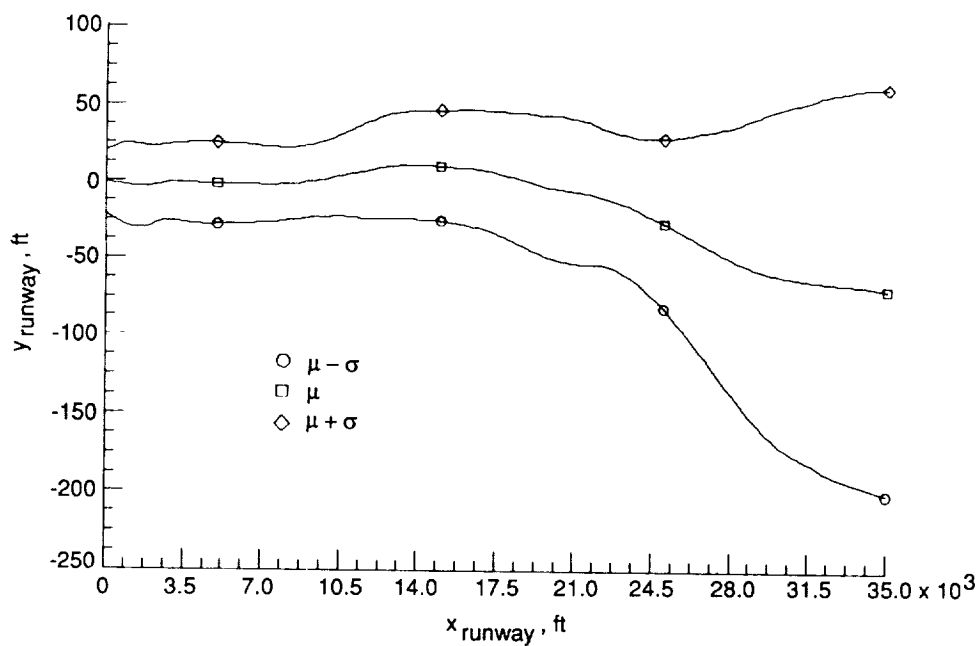
(b) Localizer deviation.

Figure 49. Mean and standard deviation of final-approach data for all runs before TIMER briefing to crew.
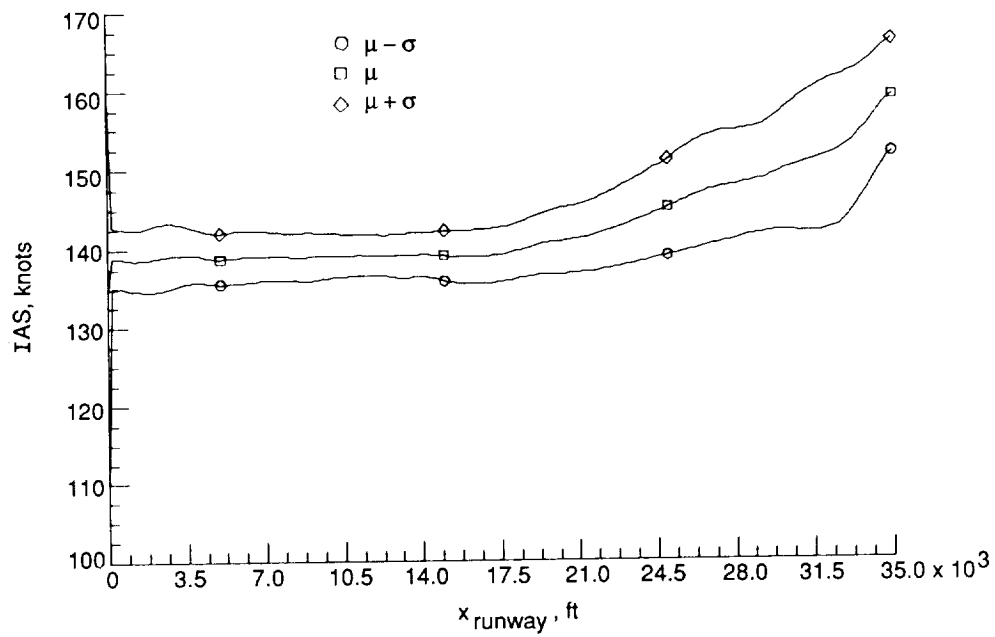
(c) Indicated airspeed.

(d) Altitude rate of change.
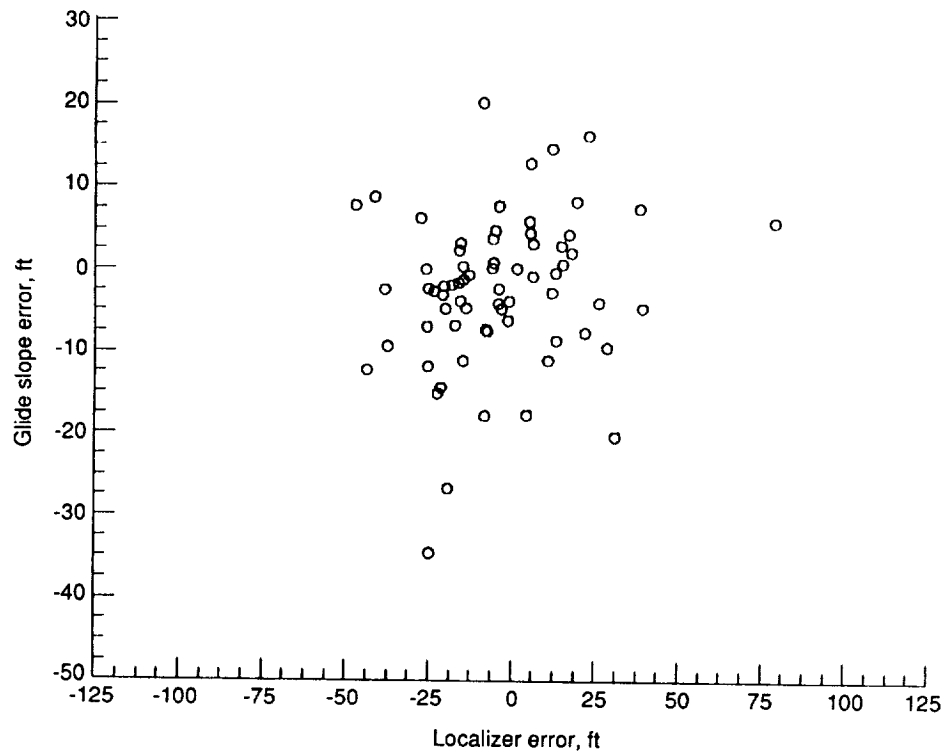
Figure 49. Concluded.

Figure 50. Glide slope and localizer errors at Category I window for all data runs.
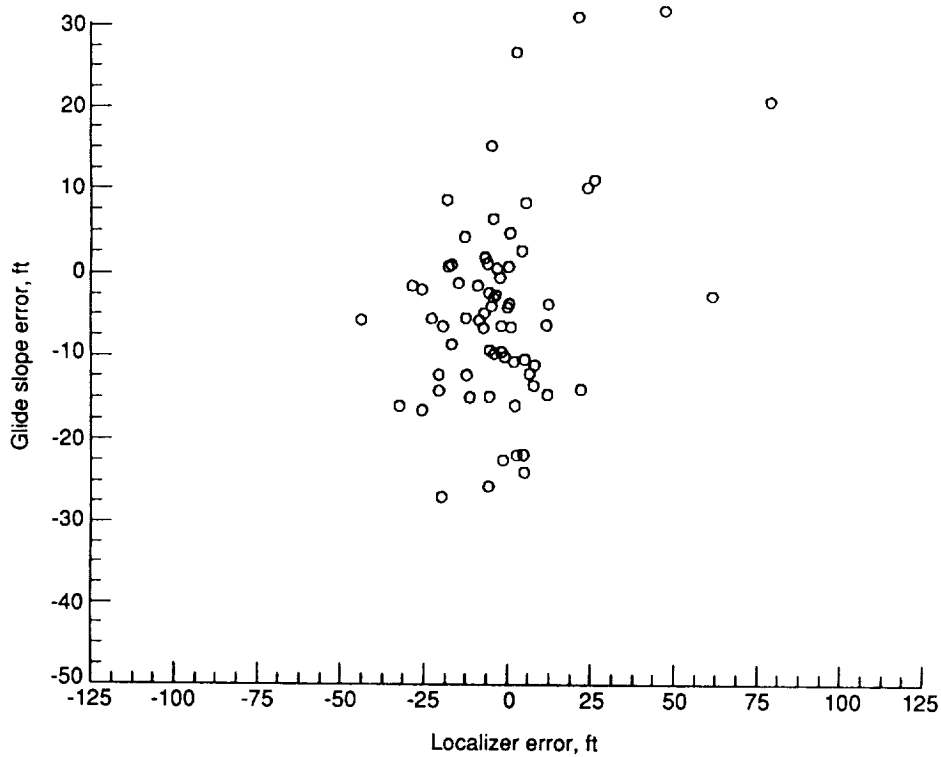

Figure 51. Glide slope and localizer errors at runway threshold for all data runs.

FLIGHT TRAJECTORY RATING SHEET

CREW NUMBER _____   DATE _____   TRAJECTORY NUMBER _____

At the end of the flight, place an X in the space that best describes your rating on each scale.
Definitions for each scale are provided on the second page for your convenience.

1. Physical Workload   Low | | | | | | | High

2. Cognitive Workload   Low | | | | | | | High

3. Perceptual Workload   Low | | | | | | | High

4. Overall Workload   Low | | | | | | | High

5. Safety   Safe | | | | | | | Not Safe

6. Passenger Acceptance   Acceptable | | | | | | | Not Acceptable

7. Skill Required   Minimum Piloting Skill | | | | | | | Maximum Piloting Skill

8. Controllability   Easy to Control | | | | | | | Hard to Control

9. Uneasiness   Not Uneasy | | | | | | | Uneasy

10. Your Performance   Satisfactory | | | | | | | Unsatisfactory

11. ATC Assessment   Identical | | | | | | | Very Different

Additional Comments:

Figure 52. Crew evaluation sheet.

57

RATING SHEET DEFINITIONS

1. **Physical Workload:**   adjusting, dialing, holding, pressing, pulling, pushing, reaching, turning, tuning, talking, writing, etc.

2. **Cognitive Workload:**   thinking, deciding, calculating, estimating, judging, checking, planning, timing, predicting, etc.

3. **Perceptual Workload:**   looking, scanning, searching, listening, feeling, noticing, comparing, identifying, matching, etc. Receiving and comprehending information through any of the senses.

4. **Overall Workload:**   combination of physical, cognitive, and perceptual workload

5. **Safety:**   Refers to your ability to control the aircraft and respond to ATC commands without jeopardizing the lives of the passengers and crew.

6. **Passenger Acceptance:**   To what extent do you think a typical passenger would find the previous flight unacceptable enough to express his/her dissatisfaction in some tangible way (complain to a member of the crew, complain to another passenger, cry out, become ill, protest to the airline, comment about the flight procedures to friends/relatives, select an alternative means of transportation for his/her next trip, etc.).

7. **Skill Required:**   How much special training or practice do you think is necessary to fly approaches/departures such as the previous flight, assuming the same avionics and flight controls?

8. **Controllability:**   How easy was it for you to follow the ATC commands during the last flight?

9. **Uneasiness:**   To what extent did you feel that the last flight placed you under pressure or subjected you to feelings of anxiety, frustration, nervousness, stress, etc.?

10. **Your Performance:**   To what extent do you think your performance during the last flight approached the best you are capable of doing? Consider whether or not you think your performance on the last flight would have been significantly better if you had had additional practice/training.

11. **ATC Assessment:**   How close to normal IFR terminal approach procedures do you judge the ATC commands and procedures to be?

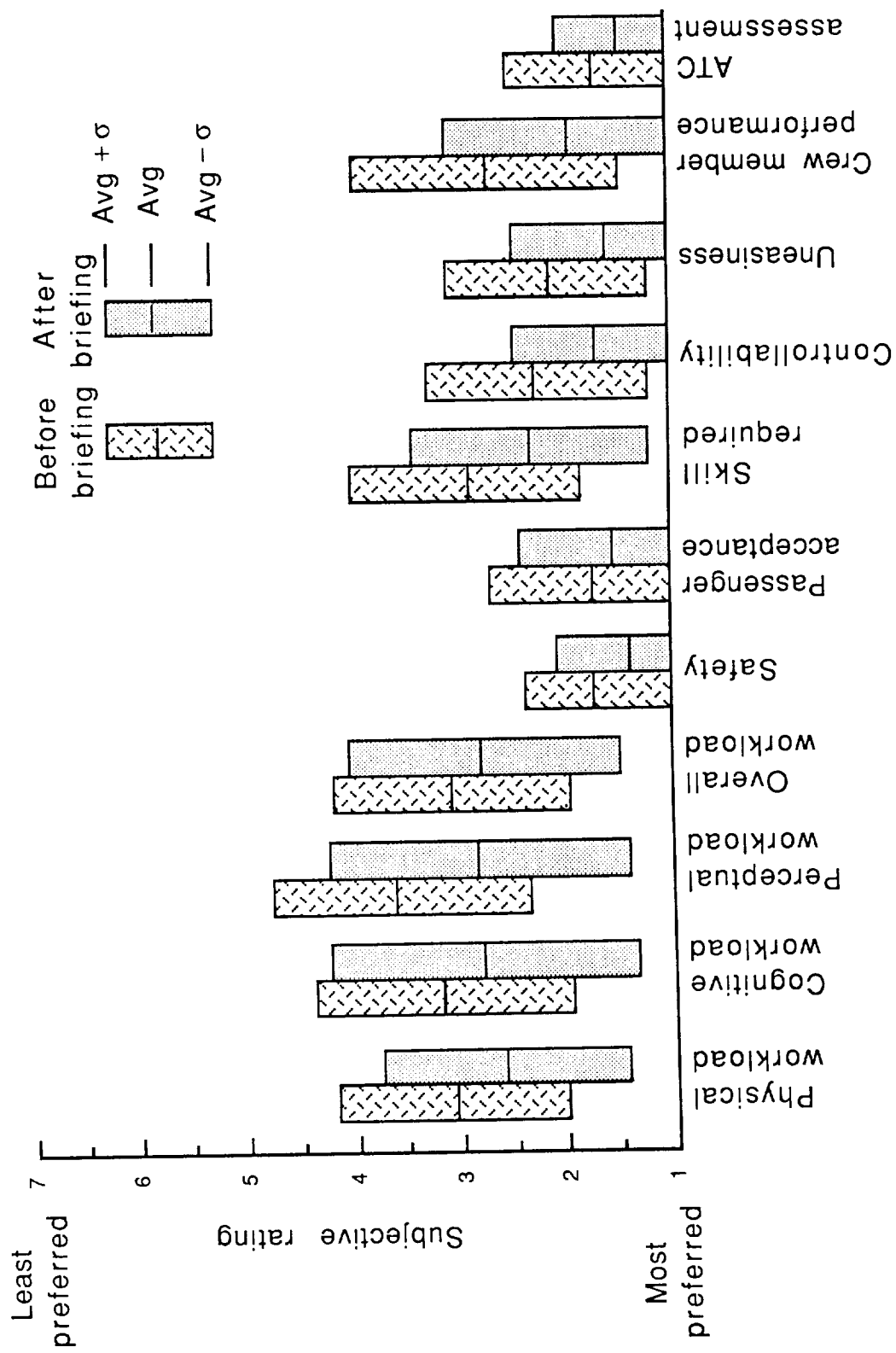Figure 53. Definition of rating categories on crew evaluation sheet.
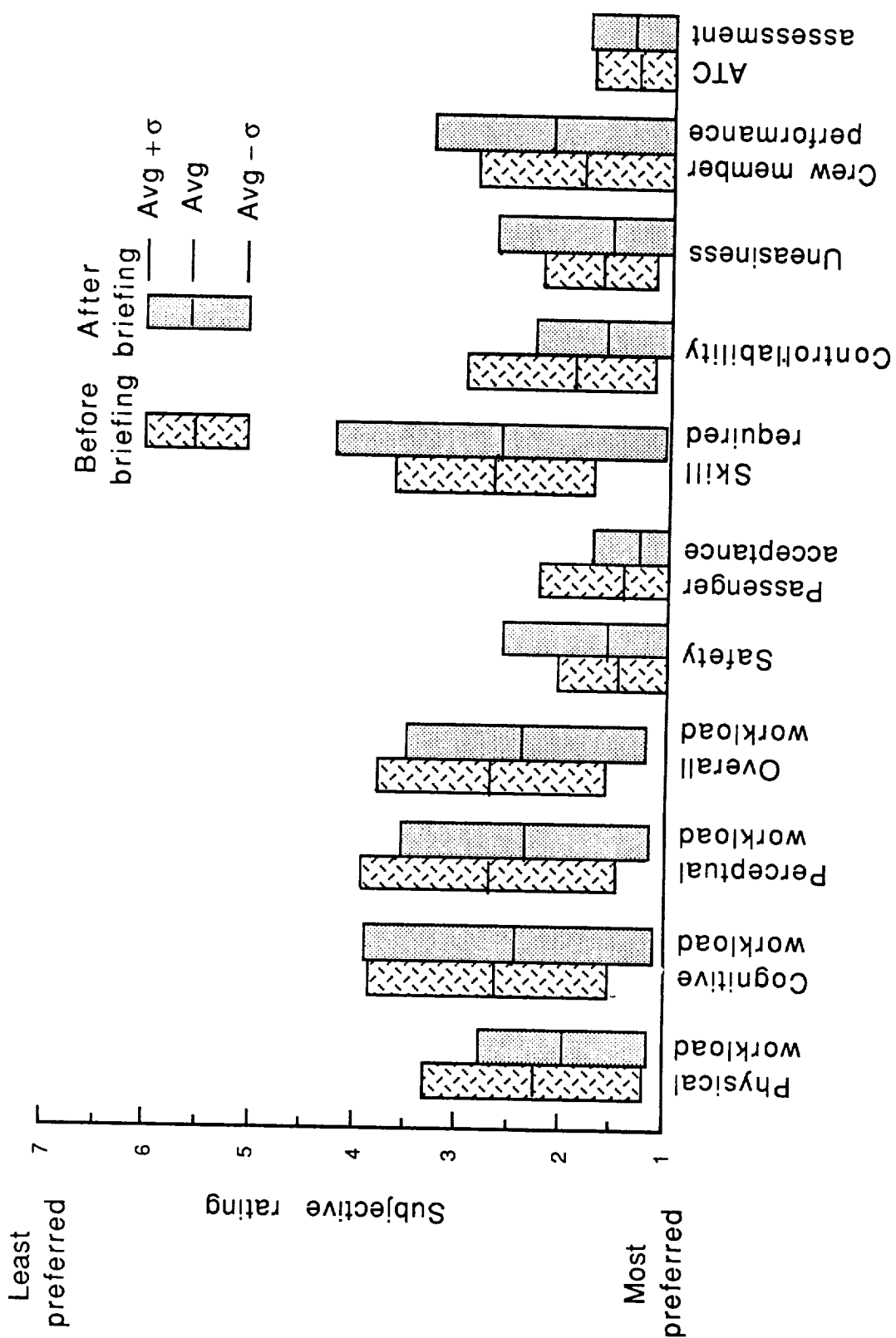
Figure 54. Subjective ratings of captains.

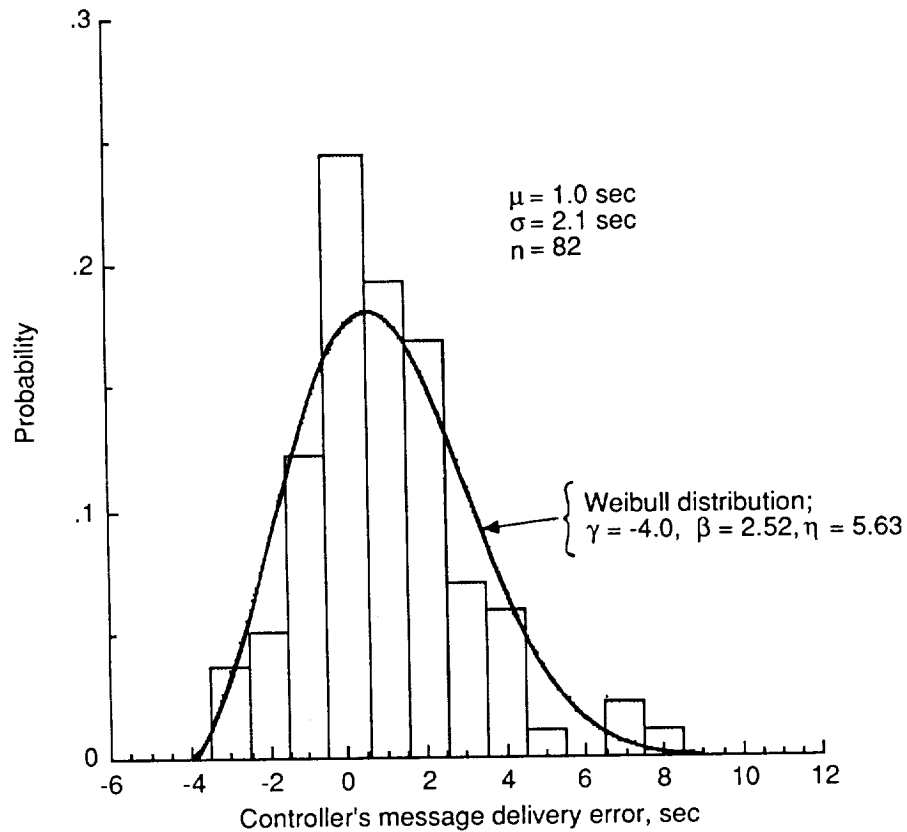Figure 55. Subjective ratings of first officers.

Figure 56. Histogram of controller's final-turn-message delivery-time error to DC-9 simulator and fitted Weibull density.
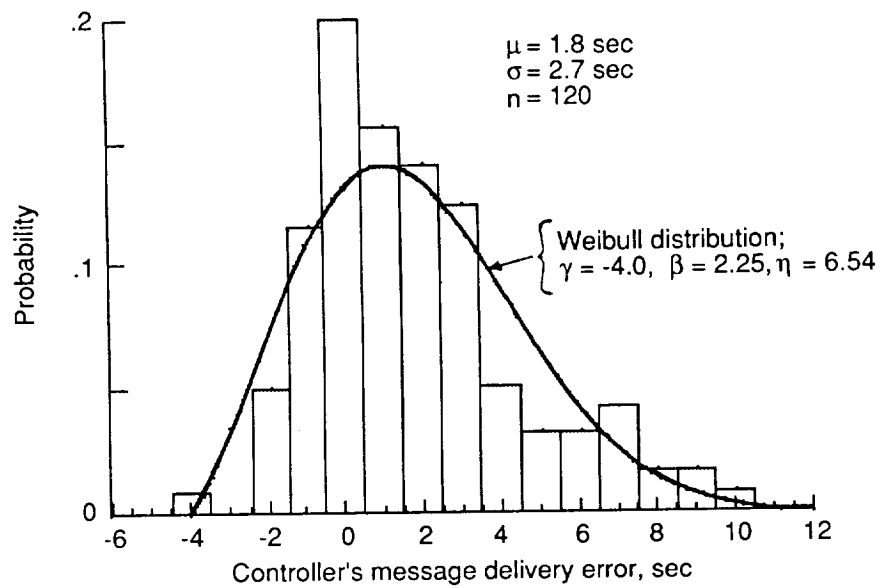

Figure 57. Histogram of controller's final-turn-message delivery-time error to TIMER-controlled aircraft and fitted Weibull density.

61

Report Documentation Page

1. Report No. NASA TP-2978	2. Government Accession No.	3. Recipient's Catalog No.

4. Title and Subtitle	5. Report Date
Delivery Performance of Conventional Aircraft by Terminal-Area, Time-Based Air Traffic Control *A Real-Time Simulation Evaluation*	April 1990
	6. Performing Organization Code

7. Author(s)	8. Performing Organization Report No.
Leonard Credeur, Jacob A. Houck, William R. Capron, and Gary W. Lohr	L-16615

9. Performing Organization Name and Address	10. Work Unit No.
NASA Langley Research Center Hampton, VA 23665-5225	505-66-41-01
	11. Contract or Grant No.

12. Sponsoring Agency Name and Address	13. Type of Report and Period Covered
National Aeronautics and Space Administration Washington, DC 20546-0001	Technical Paper
	14. Sponsoring Agency Code

16. Abstract

A description and results are presented of a study to measure the performance and reaction of airline flight crews in a full-workload DC-9 cockpit while flying in a real-time simulation of an air traffic control (ATC) concept called TIMER (traffic intelligence for the management of efficient runway scheduling). Experimental objectives were to verify earlier fast-time TIMER delivery-time precision results and obtain data for the validation or refinement of existing computer models of pilot/airborne performance. Experimental data indicated a runway-threshold, interarrival-time-error standard deviation in the range of 10.4 to 14.1 sec. Other real-time system performance parameters measured include approach speeds, response time to controller's turn instructions, bank angles employed, and ATC controller's message-delivery-time errors.

17. Key Words (Suggested by Authors(s))	18. Distribution Statement
Terminal automation Time-based air traffic control Controller aids Real-time simulation Cockpit simulation	Unclassified—Unlimited Subject Category 04

19. Security Classif. (of this report) Unclassified	20. Security Classif. (of this page) Unclassified	21. No. of Pages 66	22. Price A04

National Aeronautics and
Space Administration
Code NTT-4

Washington, D.C.
20546-0001

Official Business
Penalty for Private Use, $300

NASA

POSTMASTER: If Undeliverable (Section 158
               Postal Manual) Do Not Return